Paper Reference ID: RTC-013

TESTING METHODS IN TRIBOLOGY: A REVIEW

Umar Nirmal, Jamil Hashim, Saijod T.W. Lau

Faculty of Engineering and Technology, Multimedia University,
Jalan Ayer Keroh Lama,
75450, Melaka, Malaysia.
Tel: +606 2523007, Fax: +606 2316552
nirmal@mmu.edu.my, nirmal288@yahoo.com

ABSTRACT

This article attempts to describe some of the testing methods commonly used in tribology. It namely illustrates the contact of solid mechanics and nature of surface interaction. With the advent of sustainable development, composite materials now become more prominent in many applications. Many natural fibres in polymeric composites are being introduced in aviation industry, construction, industrial applications, automotive parts, bearing and many others, making tribo-testing more demanding. Relevant to this, the testing methods elaborated here are focused on the different types of wear test rigs used for testing of solid specimens for composite materials. Different mechanisms of wear and sliding friction of materials subjected to different wear test rigs which are built based on ASTM standards simulating the real time conditions are explained. Typical factors contributing to the wear performance of a material such as interfaces temperature (i.e. test specimen / counterface) under dry and wet tribo-testing conditions and roughness property are also detailed.

Keywords: Tribology testing methods, wear test rigs, roughness, composite material, natural fibre.

1. INTRODUCTION

Tribology is defined as the study of friction, wear and lubrication of interacting surfaces in relative motion. The importance of tribology at present time is crucial since most design applications involve 'wear and tear' process when subjected to relative motion. Medalia (1980) reported that about 63% of wear has contributed to the total cost of industries. Interestingly, these contribution factors (friction, heat, wear, etc.) cannot be eliminated completely; however, they can be minimized. According to the famous law regarding conservation of energy, it states that the total amount of energy created can never be destroyed; it can only be transformed from one state to another, for an example, kinetic energy is transformed into useful work, friction and heat dissipation to the surroundings. To link the above idea in terms of tribology, Figure 1 is presented. It illustrates two typical examples relating wear process due to relative motion; the human skeleton (c.f. Figure 1a) and the inline four stroke engine (c.f. Figure 1b). Thus, depending on the severity of the wear process, these areas (red spots) have a certain period of life span. This naturally occurring process (i.e. the decrease of output power of a car engine versus time) can be improved by means of extending its life span using tribology technology.

a) The human skeleton

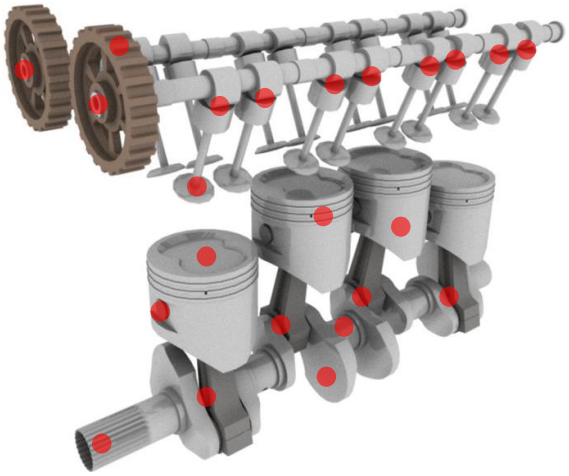

b) Four stroke inline engine
Figure 1: Typical spots on the importance of tribology

From the past decade up to present time, many researchers had introduced advance materials as a substitute to the conventionally used materials as these modified materials are excellent in wear and friction, light in weight and improved life span (El-Tayeb, 1997). For an instance, Nautiyal et al. (1983) observed that the factors responsible for wear of a piston ring sliding against cast iron combustion chamber were its surface temperature, peak combustion pressure, total energy of the wearing surfaces and other physical properties of the material under sliding. As such Dahm et al. (2003) proposed to replace the conventional piston rings with ceramic matrix nano composite piston rings as the latter had smooth wear (i.e. micro scale wear) which contributed in low wear rates during the test.

Nevertheless, new applications involving natural fibres in polymeric composites are being introduced in various areas such as housing construction materials (Hariharan et al., 2005), industrial applications (Satyanarayana et al., 1990), automotive parts fabrication (John et al., 2008), bearing applications (El-Sayed et al., 1995), structural and non-structural applications (Sreekala et al., 2002). Hence, scientific principles and calculating methods of creating new materials / composites and estimation of its wear resistance of friction nodes as well as physical simulation of friction and wear processes on a small-sized laboratory test machine need to be carried out experimentally before a proposed material/composite is commercially introduced in the market (Dahm, et al., 2003; Pogosian 1973). Prior to this, a suitable type of wear test rig should be used with appropriate parameters selected which reflect the real time application of the material/composite. Examples of this parameters are testing techniques, type of counterface used against the test samples, sliding velocities, sliding distances, applied loads, contact conditions and orientations of the test specimen with respect to the sliding direction of the counterface.

Having such knowledge, a tribo-testing machine which is capable to simulate the wear and frictional test based on the selected parameters is developed. From available published works, there are numerous types of tribo-testing machines. They differ with one another based on the suitability of the test for a specific application. Thus, the aim of this paper is to explain the various types of tribo-testing machines used in performing different types of test which reflects the real time conditions. In conjunction to that, the work further illustrates on common ways in presenting data/results upon completion of a tribological experiment/test.

2. TYPES OF TRIBO-TESTING MACHINES

2.1 Dry sand rubber wheel

(Pogosian 1973; Rajesh et al., 2002; Kim et al., 2002)

Its schematic is shown in Figure 2. It is built based on ASTM G65 standard where its recommended specimen size is 70mm x 20mm x 7mm. The rubber wheel is in contact with the specimen when a load is applied. Sand particles (i.e. fine, grain or coarse) are introduced at a certain flow rate to the rubbing zone during the test. The flow rate can be varied based on the outlet diameter of the sand hopper. Since it involves sand, the test is abrasive. Adhesive testing is possible if sand is not used. Typical application of test involves the wear performance of tire treads, bushes, bearings and rollers.

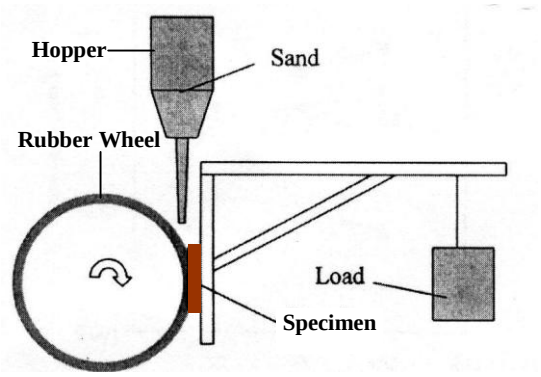

Figure 2: Schematic view of a dry sand rubber wheel wear test rig

2.2 Pin on drum
(Rajesh et al., 2002; Stevenson et al., 1996; Mutton 1978; Mutton, 1980; Blickensderfer et al., 1988)

Figure 3 illustrates the pin on drum wear test rig. It is built based on ASTM A514 standard. The specimen travels linearly with the help of the power screw while the drum rotates at a desired speed with the help of the drive chain. The speed of the specimen and the drum can be controlled by means of a speed controller incorporated at the motor system. Test can be abrasive if drum is coated with abrasive paper of different grades. Without abrasive paper, test is adhesive. Drum can be of different material (i.e. stainless steel, aluminum, cast iron, mild steel, etc) based on the suitability of the test conducted simulating the real time conditions. Application of test involves sliding of goods on rotating rollers or conveyer belts.

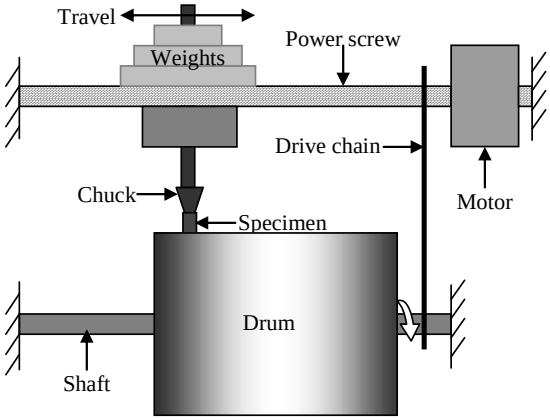

Figure 3: Schematic view of a pin on drum wear test rig

2.3 Linear tribo machine
(Yousif et al., 2010)

The schematic view of the linear tribo machine is presented in Figure 4. Its stainless steel counterface moves linearly with the help of the power screw which is directly coupled to the motor. Test can be abrasive when the stainless steel container is filled with abrasive particles, else the test is purely adhesive. A frictional indicator is connected to a load cell to measure frictional forces and a speed controller is used to vary the counterface sliding speed. Dead weights are applied parallel to the test specimen. The counterface can be of different material for different test conditions. For the adhesive test, water can be incorporated in the sliding container for the purpose of simulating the wear under wet contact conditions. Application of test involving linear tribo machine replicates the characteristics of linear sliding of window panels, doors, hinges and drawers.

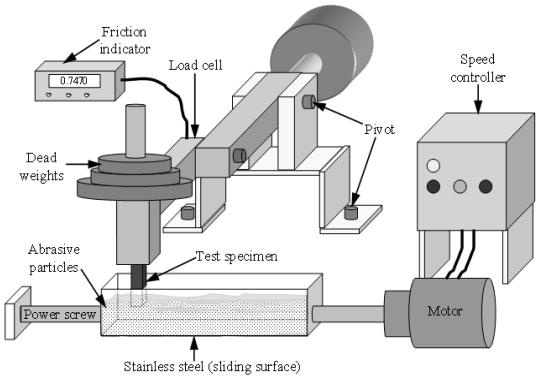

Figure 4: Schematic view of a linear tribo machine

2.4 Block on ring
(PihtIlI et al., 2002; Reinicke et al.,1998)

A schematic view of a block on ring tribo test machine is presented in Figure 5. It is built in accordance with ASTM G77, G137-95 standards. The specimen with size of 10mm x 20mm x 50mm is in contact parallel to the side of the counterface. Contact area of the test specimen subjected to the counterface is variable. A load cell is directly incorporated in the load lever of the machine to capture frictional forces during the test. A counter weight balancer is incorporated at the end of machine's load lever to balance the lever arm prior testing. This is done when no load is applied. Depending on the nature of the test, counterface can be of various types (i.e. metal, cast iron, titanium, aluminum, stainless steel, etc). Generally, this test is simulated for applications such as sliding or rolling wear behavior of tire treads, pulleys, camshafts and bearings materials.

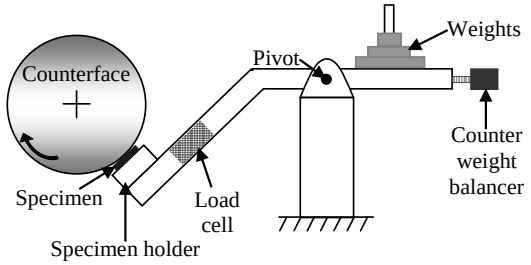

Figure 5: Schematic view of a block on ring tribo test machine

2.5 Pin on disc (Hummel et al., 2004; Mergler et al., 2004; Bijwe et al., 2002; Bijwe et al., 2001)

Its schematic view is presented in Figure 6. Built based on ASTM G99 standard, its working principle is the same as block on ring. However,

the test specimen with size of 10mm x 10mm 20mm subjected to the counterface exhibits a constant contact area throughout the test. The test specimen is set perpendicular and horizontal to the counterface. Typical application of test includes sliding wear of various materials where constant contact area of interest.

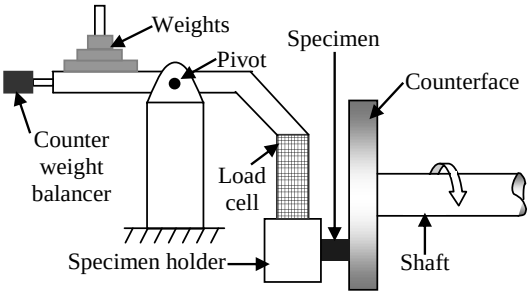

Figure 6: Schematic view of a pin on disc tribo test machine

2.6 Block on disc (Hummel et al., 2004; Mergler et al., 2004; Bijwe et al., 2002; Bijwe et al., 2001)

Figure 7 illustrates a portable block on disc tribo test machine which is built on a small scale. It is designed in accordance with ASTM G99 standard. Specimen with size of 10mm x 10mm x 20mm is subjected vertically to the counterface where the contact area is constant. A portable infrared thermometer can be incorporated to the block on disc machine for the purpose of measuring interfaces temperatures during the test. Test can be adhesive and abrasive subjected to dry sliding mode. A speed controller unit is connected to the motor to vary the counterface speed while a digital frictional indicator is connected directly to the load cell to capture frictional forces during the test.

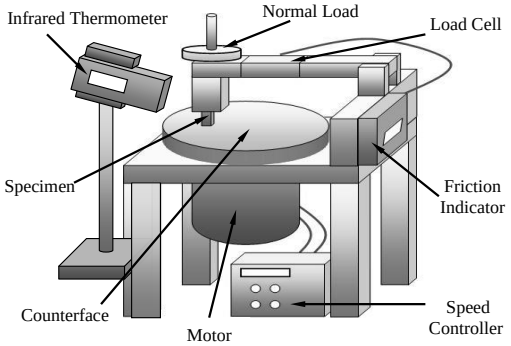

Figure 7: Schematic view of a block on disc tribo test machine

3. PRESENTATION OF DATA / RESULTS

Various methods are adopted to present / display the characteristics behaviour on wear and frictional performance of a desired material. This section summarizes some common methods on data presentation as it is mostly preferred by worldwide researchers.

3.1 Wear performance

Wear process of a material can be defined as the tendency of a material to loose weight from the removal and deformation process on the material surface as a result of mechanical action of the opposite surface due to relative motion (Hummel et al., 2004; Harsha et al., 2002). Many researchers prefer to express wear performance of a material in terms of specific wear rate. Specific wear rate can be defined as follows:

$$W_S = \frac{\Delta V}{F_n . D} \quad (1)$$

where;

W_s = Specific wear rate, $mm^3/N.m$
ΔV = Volume difference, mm^3
F_n = Normal applied load, N
D = Sliding distance, m

Therefore, the wear performance of a material is said to be superior if the specific wear rate is low (i.e. material / specimen exhibits low volume loss). However, there are a lot of other factors contributing to the wear performance of a material subjected to tribological test. Naming a few, the contact condition of the test specimen (i.e. dry / wet), orientation of the test specimen with respect to the sliding direction of the counterface and the types of reinforcements used (i.e. natural fibre / resin) are critical factors / parameters in affecting the wear performance of a material.

3.2 Frictional performance

Friction performance of a material can be defined as the force resisting the relative motion between two sliding interfaces. Generally, higher frictional performance implies the superiority of a material in exhibiting low friction coefficient values during tribological testing. Friction coefficient can be expressed as follow:

$$\mu = \frac{F_r}{F_n} \quad (2)$$

where;

μ = Friction coefficient
F_r = Friction force, N
F_n = Normal force, N

Theoretically, the component of F_r is contributed by two main elements such as adhesion force, F_a, and deformation or ploughing force, F_d (El-Sayed et al., 1995). Their corresponding relation to friction force is shown in Eq. (3).

$$F_r \approx F_a + F_d \quad (3)$$

F_a can be determined from the shear strength (τ_s) multiply with area of material contact (A); Eq. (4) (Rabinowicz 1995) while F_d is expressed in Eq. (5) (Rabinowicz 1995; Stolarski 2003; Bhushan 1999).

$$F_a = \tau_s \cdot A \quad (4)$$

$$F_d = \frac{2 \cdot F_n \cdot \tan\theta}{\pi} \quad (5)$$

where;

θ is the attack angle / roughness angle of the asperity

In summary, it can be said that from Eq. (3), (4) and (5), there are multiple factors affecting the frictional coefficient of a material. Factors such as the roughness angle of the asperity with respect to the contacting surface can be minimized when the contacting surfaces are smooth ($\theta \approx 0$). In regard to this, many reported works used various grades of abrasive sand papers to achieve a relatively smooth surface by the contacting bodies. After due research, Figure 8 proposes one possible way in achieving smooth surfaces between the test specimen and counterface before experiment start-up.

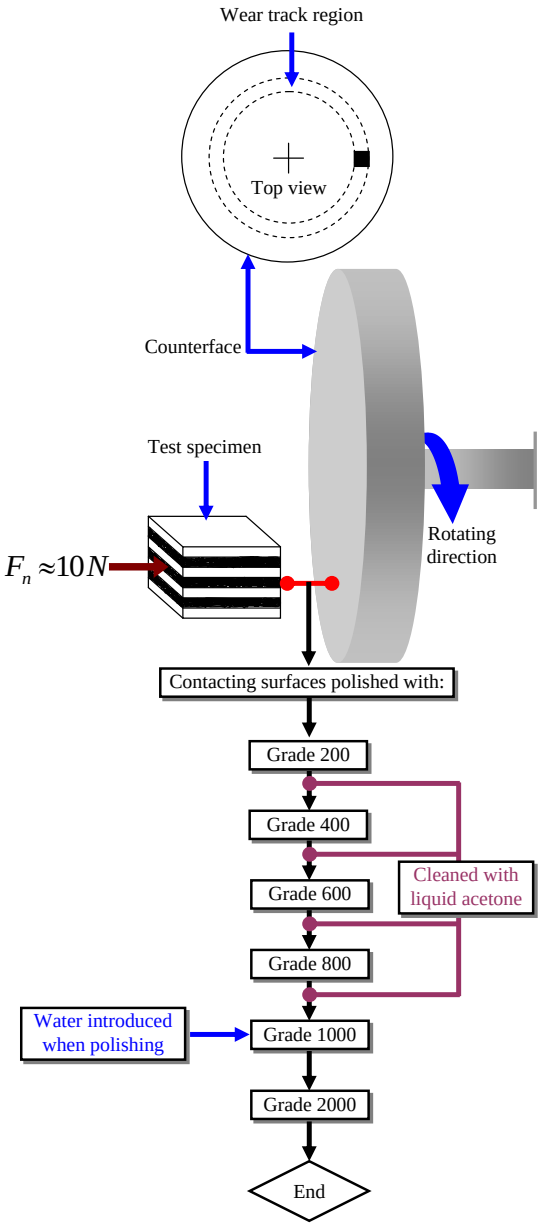

Figure 8: Proposed flow chart in achieving smooth interacting surface before experimental start-up

3.3 Temperature performance

It is important to relate/include temperature characteristics of a material when conducting tribology tests. This is because under dry adhesive wear, surface temperature of the interacting surfaces increases over time. Hence, effects of thermo-mechanical loading will be more significant on the softer phase (Bhushan 2001). This affects the wear and frictional performance of a material over long duration of experimental testing. Following to this, few techniques have been adopted in measuring temperatures during tribological test.

One of the most convenient ways is by using an infrared thermometer (Bhushan 2001). From Figure 9, an infrared thermometer is placed at a fix horizontal distance 'x' away from the test specimen. Accordingly, interfaces temperatures can be measured during the test. However, it is to be highlighted here that the accuracy of temperature measurement varies with the distance 'x'. For example, a temperature measurement at x = 1 m will differ with x = 2 m for the same test conditions. In other words, temperature measurements will be more accurate when the infrared thermometer is placed closer to the test specimen. However, the main limitation here is due to the design of the machine itself which limits the placement of the infrared thermometer close to the test specimen.

To minimize the measurement error of interfaces temperature, El-Tayeb et al., (2005) incorporated a thermocouple in an un-through hole of 2 mm in diameter which was pre-drilled on the test specimens (i.e. hole located approximately 0.75 mm above the test specimen contacting surface with counterface) during composite fabrication. Following to this, an external heat source was supplied to the counterface by means of a Bunsen burner. Concurrently, two temperature readings were recorded, i.e. from infrared thermometer and thermocouple device (c.f. Figure 10a). Based on the results obtained, a calibration graph was generated where the calibrated linear equation (c.f. Figure 10b) was used to determine the real interface temperatures. This method was reported to be more accurate (i.e. up to 90% accuracy in temperature recordings) (Yousif, et al., 2010; El-Tayeb et al., 2005; Nirmal, 2008) as compared to other measurement techniques (Chang 1983; Hanmin et al.,1987; Malay et al., 1982; Zaidi et al.,1999).

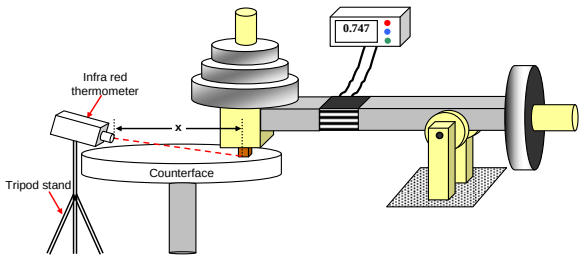

Figure 9: Incorporation of an infrared thermometer to measure interfaces temperatures

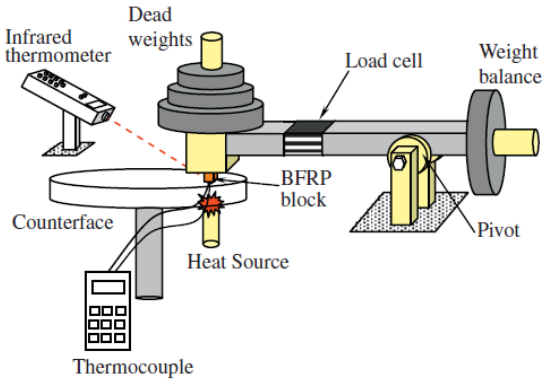

a) Temperature calibration process
(Yousif et al., 2010)

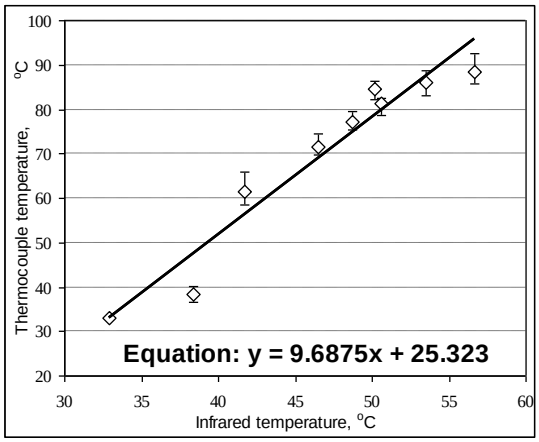

b) Corresponding calibration graph
(Nirmal, 2008)

Figure 10: Temperature calibration process with corresponding calibration graph

3.4 Roughness profile

The degree of abrasiveness to process equipment of a material subjected to tribology testing is an extensive area of study. For an instance, a tested material resulting in low abrasiveness to process equipment may contribute to an extended life span of the machine noting the fact that the material tested to be 'equipment friendly'. In conjunction to this, it is of great interest to measure surface roughness of the test specimen and the counterface before and after performing a tribological test. Surface roughness can be defined as the variations in the height of the surface relative to a reference plane. It is measured either along a single line profile or along a set of parallel line profiles. Profilometers are commonly used to measure and record surface roughness property of a material.

From available published works (Nirmal et al., 2010; Chin et al., 2009; Yousif et al., 2008), many authors prefer to express surface roughness measurement using Eq. (6).

$$R_a = \frac{a+b+c+d+.....}{n} \qquad (6)$$

where;

R_a = Roughness average, μm

$a+b+c+d+....$ = Sum of infinitesimal areas above and below the datum line, m^2

n = Length of the datum line, m

To further understand Eq. (6), a graphical illustration is presented in Figure 11. From the figure, line 'AB' is placed such a way that the sum of the areas above the line is equal to the sum of the areas below the line. Therefore, a Profilometer working principle is to measure the penetration depth formed by the asperities and local valley thereby producing the roughness average (Ra) value. However, there are also different ways of expressing the roughness property of a material. They are summarized in Table 1.

Table 1: Methods in expressing roughness property of a material

Symbol	Brief description
R_q	Root mean square average
R_{sk}	Skewness average
R_{ku}	Kurtosis average
R_t	P-V distance average (P-V: highest asperity to the lowest valley found anywhere along the profile length)
R_p	Maximum P-M distance average (P-M: height of the highest asperity and the mean line within one sampling length)
R_v	Maximum valley depth average
R_z	Average peak to valley height
R_{pm}	Average peak to mean height
R_{mr}	Material ratio average
R_k	Core roughness depth average
R_{pk}	Reduced peak height average
R_{vk}	Reduced valley depth average

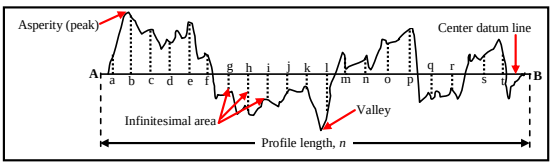

Figure 11: Graphical illustration in determining roughness average, Ra

4. CONCLUSION

The various types of tribo-testing machines, their accessories and applications have been discussed. They differ with one another on the basis of the suitability of the test for specific application. The sole purpose of the various types of tribo-testing machines is to establish the wear performance of materials in real time conditions. There are several factors contributing to tribology testing such as friction coefficient and wear performance of materials, surface roughness of a material/counterface and the degree of abrasiveness of a material. Understanding tribological factors such as roughness angle of the asperity with respect to the contacting surface and their effect on wetness and heat are valuable in assessing the quality of contact; i.e. test specimen against the counterface. Materials with low specific wear rate are considered to be superior (i.e. high wear resistance), while low abrasiveness to process equipment implies a longer extended life span of a particular material.

REFERENCES

Bhushan, B 1999, *Principles and applications of tribology*, Wiley, New York.

Bhushan, B 2001, *Modern Tribology Handbook*, CRC Press.

Bijwe, J, Indumathi, J & Ghosh, AK 2002, 'On the abrasive wear behaviour of fabric-reinforced polyetherimide composites', *Wear*, vol. 253, no. 7-8, pp. 768-77.

Bijwe, J, Indumathi, J, John Rajesh, J & Fahim, M 2001, 'Friction and wear behavior of polyetherimide composites in various wear modes', *Wear*, vol. 249, no. 8, pp. 715-26.

Blickensderfer, R & Laird III, G 1988, 'A pinion–drum abrasive wear test and comparison to other pin tests', *J. Test. Eval.*, vol. 16, pp. 516–26.

Chang, HW 1983, 'Wear characteristics of composites: Effect of fiber orientation', *International Journal of Wear*, no. 85, pp. 81-91.

Chin, CW & Yousif, BF 2009, 'Potential of kenaf fibers as reinforcement for tribological applications', *Wear*, vol. 267, no. 1550-1557.

Dahm, KL, Panagopoulos, K & Dearnley, PA 2003, 'The wear response of ceramic matrix nano-composite coatings in simulated piston-ring/cylinder wall test environments', in MPGDaAAL D. Dowson (ed.), *Tribology and Interface Engineering Series*, Elsevier, vol. Volume 41, pp. 511-5.

El-Sayed, A, El-Sherbiny, MG, Abo-El-Ezz, AS & Aggag, GA 1995, 'Friction and wear properties of polymeric composite materials for bearing applications', *Wear*, vol. 184 no. 1, pp. 45-53.

El-Tayeb, N 1997, *Science of Tribology, Friction, Wear, and Lubrication*, 2nd Edition edn, Egypt Publishing Company.

El-Tayeb, NSM, Yousif, BF & Brevern, PV 2005, 'On The Effect Of Counterface Materials On Interface Temperature And Friction Coefficient Of GFRE Composite Under Dry Sliding Contact', *American Journal of Applied Sciences*, vol. 2, no. 11, pp. 1533-40.

Hanmin, Z, Guoren, H & Guicheng 1987, 'Friction and wear of poly (phenylene sulphide) and its carbon fiber composites: I. Unlubricated', *International Journal of Wear*, no. 116, pp. 59-68.

Hariharan, ABA & Khalil, HPSA 2005, 'Lignocellulose-based Hybrid Bilayer Laminate Composite: Part I - Studies on Tensile and Impact Behavior of Oil Palm Fiber-Glass Fiber-reinforced Epoxy Resin', *Journal of Composite Materials*, vol. 39, no. 8, pp. 663-84.

Harsha, AP & Tewari, US 2002, 'Tribo performance of polyaryletherketone composites', *Polymer Testing*, vol. 21, no. 6, pp. 697-709.

Hummel, SR & Partlow, B 2004, 'Comparison of threshold galling results from two testing methods', *Tribology International*, vol. 37, no. 4, pp. 291-5.

John, MJ & Thomas, S 2008, 'Biofibres and biocomposites', *Carbohydrate Polymers*, vol. 71, no. 3, pp. 343-64.

Kim, YS, Yang, J, Wang, S, Banthia, AK & McGrath, JE 2002, 'Surface and wear behavior of bis-(4-hydroxyphenyl) cyclohexane (bis-Z) polycarbonate/polycarbonate-polydimethylsiloxane block copolymer alloys', *Polymer*, vol. 43, no. 25, pp. 7207-17.

Malay, K & Bahadur, K 1982, 'An investigation of the temperature rise in polymermetal sliding', *International Journal of Wear*, no. 82, pp. 81-92.

Medalia, AI 1980, 'On structure property relations of rubber', paper presented to Proc. Int. Conf., Kharagpuur.

Mergler, YJ, Schaake, RP & Huis, VAJ 2004, 'Material transfer of POM in sliding contact', *Wear*, vol. 256, no. 3-4, pp. 294-301.

Mutton, PJ 1978, *High stress abrasion testing of wear resistant steels and cast irons*, Broken Hill Proprietary, Melbourne, Clayton, Victoria, Australia.

Mutton, PJ 1980, *High stress abrasion testing of wear resistant materials*, 1, Broken Hill Proprietary, Melbourne Res. Lab, Clayton, Victoria, Australia.

Nautiyal, PC, Singhal, S & Sharma, JP 1983, 'Friction and wear processes in piston rings', *Tribology International*, vol. 16, no. 1, pp. 43-9.

Nirmal, SG 2008, 'An Investigation of Wear and Frictional Performance of Betelnut Fiber Reinforced Polyester Composite Under Dry Contact Condition', Multimedia University.

Nirmal, U, Yousif, BF, Rilling, D & Brevern, PV 2010, 'Effect of betelnut fibres treatment and contact conditions on adhesive wear and frictional performance of polyester composites', *Wear*, vol. 268, no. 11-12, pp. 1354-70.

PihtIlI, H & Tosun, N 2002, 'Effect of load and speed on the wear behaviour of woven glass fabrics and aramid fibre-reinforced composites', *Wear*, vol. 252, no. 11-12, pp. 979-84.

Pogosian, AK 1973, 'Forecasting the viability of friction pairs in accelerated tests', *Wear*, vol. 26, no. 2, pp. 175-86.

Pogosian, AK 1977, *Friction and Wear of Filled Polymer Materials*, Moscow.

Rabinowicz, E 1995, *Friction and Wear of Materials*, John Wiley and Sons, New York.

Rajesh, JJ, Bijwe, J & Tewari, US 2002, 'Abrasive wear performance of various polyamides', *Wear*, vol. 252, no. 9-10, pp. 769-76.

Reinicke, R, Haupert, F & Friedrich, K 1998, 'On the tribological behaviour of selected, injection moulded thermoplastic composites', *Composites Part A: Applied Science and Manufacturing*, vol. 29, no. 7, pp. 763-71.

Satyanarayana, KG, Sukumaran, K, Mukherjee, PS, Pavithran, C & Pillai, SGK 1990, 'Natural fibre-polymer composites', *Cement and Concrete Composites*, vol. 12, no. 2, pp. 117-36.

Sreekala, MS, George, J, Kumaran, MG & Thomas, S 2002, 'The mechanical performance of hybrid phenol-formaldehyde-based composites reinforced with glass and oil palm fibres', *Composites Science and Technology*, vol. 62, no. 3, pp. 339-53.

Stevenson, ANJ & Hutchings, IM 1996, 'Development of the dry sand/rubber wheel abrasion test', *Wear*, vol. 195, no. 1-2, pp. 232-40.

Stolarski, TA 2003, 'Modern Tribology Handbook: Vol. 1-Principles of Tribology, Vol. 2- Materials, Coating, and Industrial Applications, Editor-in-Chief: Bharat Bhushan, CRC Press 2001', *Tribology International*, vol. 36, no. 7, pp. 559-60.

Yousif, BF & El-Tayeb, NSM 2008, 'Adhesive wear performance of T-OPRP and UT-OPRP composites', *Tribology Letters*, vol. 32, pp. 199-208.

Yousif, BF, Lau, STW & McWilliam, S 2010, 'Polyester composite based on betelnut fibre for tribological applications', *Tribology International*, vol. 43, no. 1-2, pp. 503-11.

Yousif, BF, Nirmal, U & Wong, KJ 2010, 'Three-body abrasion on wear and frictional performance of treated betelnut fibre reinforced epoxy (T-BFRE) composite', *Materials & Design*, vol. 31, no. 9, pp. 4514-21.

Zaidi, H & Senouci, A 1999, 'Thermal tribological behavior of composite carbon metal/steel brake', *International Journal of Wear Applied Surface Science*, vol. 144-145, pp. 265-71.

Paper Reference ID: RTC 024

TRIBOLOGICAL ASPECT OF RESIN IMPREGNATED GUNNY AND RESIN REINFORCED HONEYCOMB FOR BODY SHELL APPLICATIONS

R. M. Nasir, M. R. A. Montaha

School of Mechanical Engineering, Universiti Sains Malaysia,
14300 Nibong Tebal,
Seberang Perai Selatan, Pulau Piang, Malaysia.
E-mail: meramdziah@eng.usm.my

ABSTRACT

This paper present an attempt to use gunny fibre & honeycomb polymer as reinforced for tribo-composite based on polyester for tribological application. Resin impregnated gunny (RIG) , polypropylene honeycomb (PPHC) and resin reinforced honeycomb (RRHC) was fabricated using hand-lay-up and cold press techniques. Wear rate, frictional behaviour of both material were studied against polished stainless steel counter face using pin-on-disk (POD) machine at different applied load (5-25 N) and sliding velocity (1.12 – 22.56 m/s). In general specific wear rate increases as increasing load and velocity. The specific wear rate for RIG is lower than RRHC and PPHC at increasing load for approximately 0.35 mg/N and comparable at increasing velocity approximately 0.16 mg/N. The highest specific wear rate for RIG and RRHC is at 10N and 20N respectively indicating the wear endurance for load is better performed in RRHC compared to PPHC and RIG. Friction was minimum value at 0.01 for both RIG and RRHC but PPHC catastrophic failure. Compression result also showed that the presence of gunny fibre as reinforcement shows highest load more than 8N comparing to RRHC and PPHC which is less than 1N. The average maximum displacement is highest for RRHC at 1.8 cm while that for RIG and PPHC is at 1.6 and 0.9 cm respectively. Finally the worn surface morphology of both materials were studied using scanning electron microscope (SEM) in relation to external deformation.

Keywords: Abrasion, Friction, Resin Impregnated Gunny, Resin Reinforced Honeycomb

1. INTRODUCTION

In the era of recycle, reuse and reduce, gunny was chosen as it is reliable and recyclable. Rahman et al. (2008), suggested natural gunny from treated woven jute is the cheapest lignocellulosic long vegetable bast fiber and abundantly available in Bangladesh to be used for fibre due to its strength and durability. Besides gunny, they were used for making ropes, shopping bags, floor mates and many other applications. The major drawback factor using jute fiber as reinforcing material is its hydrophilic nature that responsible for moisture absorption and consequently deformation of the product. Therefore, some chemical treatment to improve its hydrophilic nature and mechanical properties needed in order to reduce damage in jute fibre. Beside jute is a potential natural rubber to replace synthetic fibers due to its lightweight, easy processing, renewable, recyclable, reusable leading to material efficiency and most importantly; cost effective. In addition, they are biodegradable and do not leave residue or result in by-product that are toxic.

In the current work, raw jute fiber was oxidised with sodium periodate and manufactured composites were post-treated with urotropine to increase the compatibility of the jute fiber with PP (polypropylene) matrix. For RRHC, honeycomb made from polypropylene, and they are synthetic polymers. Nowadays, various reinforcing fillers are combining with synthetic polymer in order to improve the mechanical properties to fulfill the actual application demand characteristic. The polymer based material is preferred in these current years over metal-based counterparts in view of their low coefficient of friction light weight material and ability to sustain loads as mentioned by Quintelier et al.(2006). Polymer is extensively used in the sliding components such as gears and cams where their self lubricating properties are exploited to avoid the need for oil or grease lubrication with its attendant problem of

contamination as stated by Unal et al. (2004). Although from above statement using natural fibre is better compare to synthetic polymer, but from triblogy point of view, it phenomenon might be different. It is known that surface topography, contact condition (sliding velocity, load, temperature, sliding distance and contact geometry), and humidity have been recognized as a source of scatter factor that can affect the experiment. Other such as in dynamic parameters of the friction test apparatus; like the pin must translate back and forth in parallel to the load axis to stay in contact with the disk if there is a misalignment or distortion in the face of the disk also contribute to the variable factors. However, the factors that being manipulated in this work focusing only on three parameters; disk velocities, pin load and sliding distance. Others than that, precaution steps were taken into account so that it will be constant factor for repeated experiment.

According to Holmberg et al. (1987), in dry contact abrasion condition, wear rate reduction is effective for adhesion and fatigue wear. This wear reduction is base on the fibre load carrying capacity, their higher creep resistance and thermal conductivity. Material for pin and disk must also be consistence, stainless steel counter surface and the experiment was carried out at room temperature and humidity. For manipulative factor, higher load make fibre more sensitive to breaking and pulverizing. El-Tayeb et al. (1996) stated that the volumetric wear rate will increase with increasing applied load and increasing sliding distance. Godfrey(1995) also suggested that for disk velocity, normal force oscillation increase as speed increase in POD test. This is supported by Nasir et al. (2011) said that sliding velocity exerts greater influence on the sliding wear than applied load. Past research show that polymer sliding speed of wear does not always follow the usually accepted engineering rule of "higher sliding, the higher wear rate". Due to another researcher, Acilar et al. (2004) overruled that sliding speed should be sufficiently low in order to contain the temperature rise of the polymer used, because this temperature rise effect in a significant increase in the friction coefficient values.

During testing, unwanted vibration may arise. During operation of machine vibration and chattering are costly in terms of reduction of performance and service life, and sometimes endangering equipment and personel as stated by Yoon et al. (1997). Commonly, oscillation was observed in recording friction force during unlubricated or boundary-lubricated POD wear test. The result validity lays in how to report properly friction coefficient data in such a way that information about stability and uniformity of sliding is correctly represented. A nominal value is not enough to represent the data; a range of values should be reported as.

In order to detect friction oscillation, speed of the chart recorder must be increase, use an oscilloscope, a computer data acquisition program or slow down the disk rotation speed. On the other hand, very low disk speed may eliminate friction oscillation. It is because as mechanics analyses have clearly shown, normal force oscillations increase as speed increase in POD wear test. Therefore, slowing down the disk rotation rate changes the dynamics of the system and in some systems may tend to suppress oscillation, at least until very low speeds, when stick-slip processes may set in. From previous research on data dispersion in POD wear test showed dispersion in the range of 28-47% and 32-56% for disk and pin respectively. For the disk, the dispersion increase when decrease both sliding speed and applied load, for the pin, no clear relation was found said Yousif et al. (2010). Commercial disk and pins were used in this test to eliminate the influences of any particular laboratory preparation and with intention of reproducing as closely as possible a potential industry type of sliding coupling.

For the experiment of physio-mechanical properties improvement of jute fiber reinforced polypropylene composites by post-treatment give interesting result. The researcher conclude that tensile strength of the composites decrease with an increase in jute fiber loading. However, for 20% post-treated jute reinforced composite give higher tensile strength compared to the PP alone. It was also proposed that optimum set of mechanical properties using 30% jute fibre reinforce PP composite, compare with other manufactured composite. So bonding between the jute fibre and PP matrix improve the mechanical properties at higher fibre content. The present pre and post-treatment of jute reinforced polypropylene composite are adequate at research level but not for commercial exploitation due to weight as mention by Rahman et al. (2008).

Base on wear test mechanism of glass fiber reinforced polyester composite subjected to sliding wear for load ranging from 60-300N at a constant speed are studied by Quintelier et al. (2006) using Scanning Electron Microscope (SEM). Under dry condition, the related conclusion made, that the friction force are dependable both on the production of the thin

polymer film on the wear surface and orientation of the fibre, whereby parallel orientation give lower friction and transverse orientation give higher friction. The effect of fibre as reinforced on the wear leads to a fibre related wear track. Final curvature of the wear track was determined by the fibre.

For research specifically for polymers in friction and wear test, the point that must be focused are coefficient of friction in the range 0.13-0.63, while specific wear rates in the range $5x10^{-16}$ – $2.1x10^{-14}$ mg/N for 22 commercially available polymer material. A decreasing of ambient temperature (until -35 °C) is reducing the coefficient of friction and wear rates for most of the materials. The polyester itself had low coefficient of friction but showed a considerable variation in wear rate as observed by Yoon (1997) earlier.

A polyester composite based on betelnut fibre was fabricated and tested for tribological applications at different applied load and sliding distance at specific sliding velocity under wet and dry contact condition. The result show that wet condition give better wear and frictional performance of betelnut fibre reinforced polyester (BFRP) compare to dry condition. The tensile strength is reduced about 17% at wet condition but in the other hand has higher strain, about 26% compare to dry. Thus the wear and frictional performance of BFRP composite improve about 54% and 94% respectively when water presence by Yousif which is very promising in order to reduce wear rate and frictional force for future work.

Meanwhile, the use of pin-on-disk as studied by Nair et al. (2009) was pushed to new limits by developing unique applications to cover a variety of testing parameters. Harsha et al. (2003) presented three case studies; comparison of different ice melting compound, high temperature testing of TiN coats and electrical contact resistance of polypropylene coating. All cases are unique example to showed in order to obtain more accurate representation of friction and wear properties, user can simulate true in service condition on tribological test as supported by Guicciardi et al. (2002) study.

2. EXPERIMENT

2.1 Selected materials

Gunny

RIG was chosen because of gunny itself can be biodegradation and beneficial properties like light in weight, reduce wear in machine component, easy to found, renewable source and also cheap in price plus its high specific strength. These properties were suitable enough for today world that aware of green world concept in real life situation. The gunny used is as shown in Fig. 1.

Figure 1 Gunny used

Honeycomb

RRHC was chosen base on polymer which have less friction force, light weight component, high strength, have the ability to overcome weight load and also self lubricating and healing. Honeycomb shape give beneficial properties like light, strong and quiet consistence hexagonal shaped. It's light in weight due to hexagonal structure that needs minimum material to produce some other shape, a plate, compare to solid plate itself. It's quiet because polypropylene honeycomb (PPHC) that acting as sound damping materials due to PP viscoelasticity and cell structure that can be vibration damped, sound absorption and also sound insulation. The honeycomb structure is shown in Fig.2.

Figure 2 PPHC materials used

Resin and Hardener

Resin was used to impregnated gunny and to reinforced honeycomb. The resin that be used is polyester. Polyester has some advantages like easy to use and lowest cost of resin available. For hardener that be used is MEKP (methyl ethyl ketone peroxide), the hardener was used as catalyst to polyester to short the cure time.

2.2 Fabrication of specimen

For RIG, hand lay-up technique was used; the gunny laid with resin and sandwiched with aluminium sheets. The specimen has a dimension of 210 (a) x 297(b) x 10mm(c) cut into specific sizes. Then, gunny pieces were layer up by resin one by one, until fourth pieces. The resin must be uniformly distributed on the gunny pieces. Combination of gunny and resin call Resin Impregnated Gunny (RIG).Then, another sheet of aluminum foil was used to cover the RIG, and compressed by some load from brick to make sure the RIG will cure uniformly. After several hour (6-7hours), the RIG ready to take out from the sheet of aluminum.

For RRHC, there is much simpler way to make it. First, upper layer of PPHC need to be removed and replace with sheet of tissue. Then, the resin was distributed on top of the PPHC, uniformly. The combination of resin with PPHC became resin reinforced honeycomb (RRHC). After several hour, the RRHC ready to next stage, tested with mechanically and tribologically.

Material dimensional specifications is shown in Table 1 for respective tests.

Table 1: Material specifications

Test		**Material Specification** (length x width x depth)
Mechanical	Hardness (Rockwell)	20x40x6 mm
	Compression	20x23x6 mm
Tribology	POD	20x10x6 mm
Optical	SEM	Base on above specimen

2.3 Mechanical test

There only 2 test under mechanical test; hardness and compression test. For hardness test, Rockwell machine was used for only on RIG material. It's because RRHC and PPHC itself not suitable for this test due to plastic properties. Rockwell machine was set on /18 mild steel ball, 60kgf in Scale F for specimen hardness.

For compression test, Instron Table Mounted Universal Testing Machine was used, set under certain specification. For this testing, it was set up on 10 mm/min velocity, rectangular material tested shape and 10 mm in displacement.

2.4 Tribology test

For tribology test, wear test, the machine that was used are Pin-on-disk (POD). The original concept is measure specimen weight, before and after wear. The ranges of normal load are 5N until 35 N or until severely wear, and sliding velocity ranges from 1.12 m/s up to– 22.56 m/s.

Figure 3 Set up of POD Machine

This test was doing investigation on wear and friction characteristic on RIG and RRHC under dry condition against polished stainless steel counter face. The set up was basically as shown as Figs. 3 and 4:

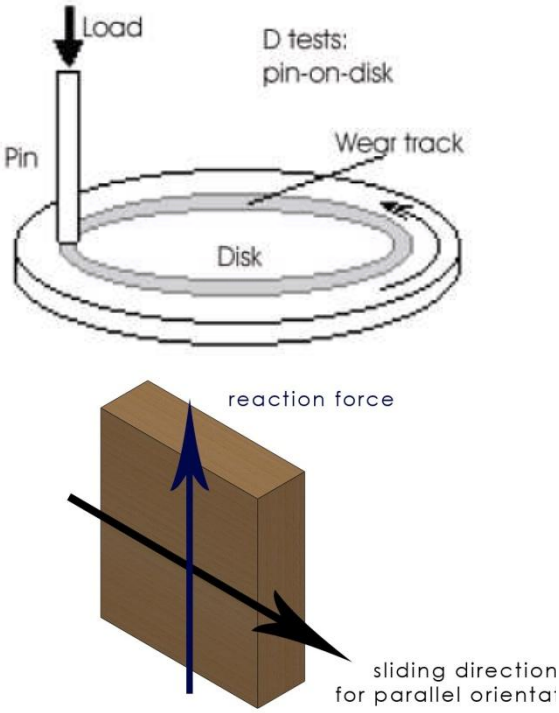

Figure 4 Schematic illustration showing the specimen of RIG

2.5 Qualitative test

After above test was done, the specimen was analyzed by using bio-rad Alicona SEM machine to see the changes of microstructure.

3. RESULTS AND DISCUSSION

3.1 Compression test

For RIG, the specimen was cut into 20x23x10 mm for compression test. 5 unit of RIG specimen was used and here the graph load versus displacement. Fig. 5 shows the specimen after compression test. From the five experiments carried, the average maximum value load for RIG compression test is 8.05 N at 1.57 cm. For PPHC and RRHC compression test, the specimen became as shown in Figs. 6 and 7.

Figure 5 RIG specimen after compression test

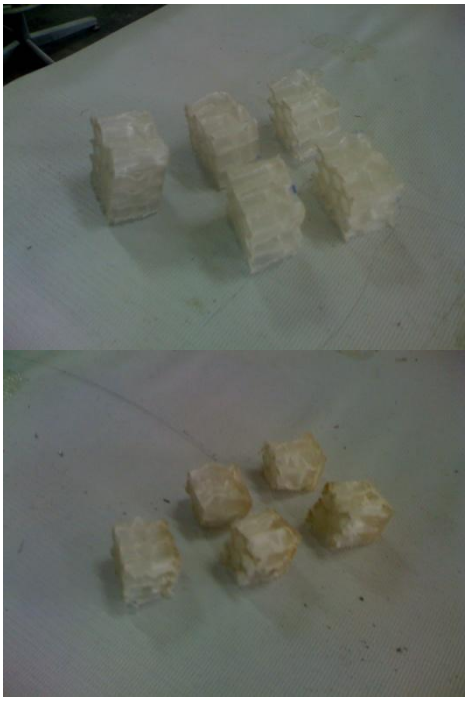

Figure 6 PPHC specimen after comp. test
Figure 7 RRHC specimen after comp. test

The compression results are shown in Figs. 8 through 10 for RIG,PPHC and RRHC respectively. From both graph (Figs. 8 and 9), it shows some increasing after decreasing in load applied, which means, both PPHC and RRHC have some recovery after the specimens exceed maximum load the specimen can sustained, compare to RIG, the graph continue to decrease after maximum load was applied, which means RIG does not have recovery ability.

From the 5 experiment carried out, the average maximum value load for PPHC compression test is 0.44 N at 0.87 cm displacement, and for RRHC compression test is 0.99 N at 1.79 cm displacement, base on Figs. 9 and 10 respectively.

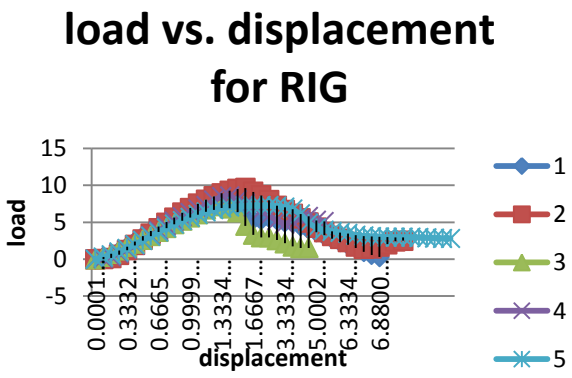

Figure 8 Effect of load on displacement for RIG

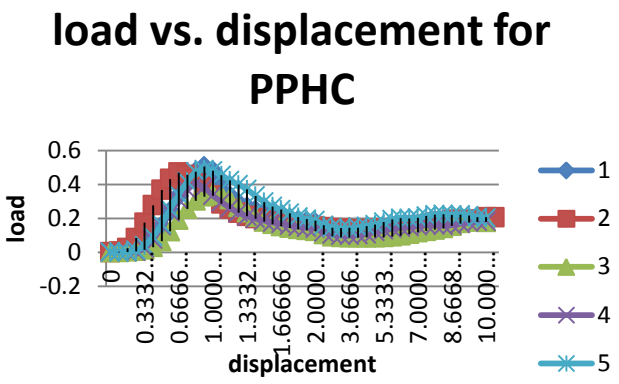

Figure 9 Effect of load on. displacement for PPHC

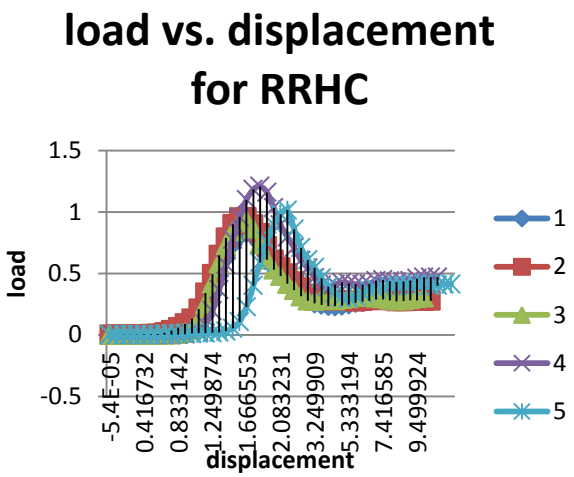

Figure 10 Effect of load on. displacement for RRHC

From Figs. 8 to 10 the data accumulated was extracted and simplified in Tables 2 and 3 for the all specimens. From both tables, RIG gave highest maximum loading compare to the others and RRHC gave highest maximum displacement.

Table 2: Average max load data for RIG, RRHC and HC

Material	Maximum load data (N)					Average max load (N)
RIG	7.486248	9.622024	7.342972	8.562843	7.255141	8.0538456
RRHC	1.014006	1.208199	0.926933	0.955662	0.831223	0.9872046
PPHC	0.506072	0.470081	0.341891	0.401715	0.486568	0.4412654

Table 3: Average max displacement data for RIG, RRHC and HC

Material	Maximum displacement data (cm)					Average max disp (cm)
RIG	1.250035	1.583356	1.583303	1.66666	1.749963	1.5666634
RRHC	2.166588	1.833321	1.666606	1.666606	1.666553	1.7999348
PPHC	0.916553	0.666643	1.000017	0.833357	0.916553	0.8666246

3.2 Hardness test

This test only carried out by RIG specimen due to material suitability, which means elastic material like RRHC is not suitable as the reading for hardness fluctuated when both PPHC and RRHC due to self-healing property whereby HC tend to recover to its original shape. Therefore the average hardness value for RIG is 66HRF.

3.3 Wear test

Effect of wear on RIG

For RIG, the specimen was cut into 20x10x6 mm for wear tests. Ranges of velocity (1.12m/s – 22.56m/s) and ranges of loads (5N - 25N) were used:

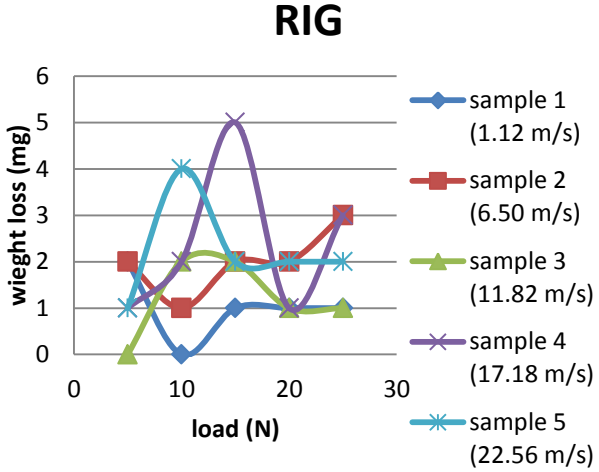

Figure 11 Effect of weight loss vs. load for RIG for different velocity

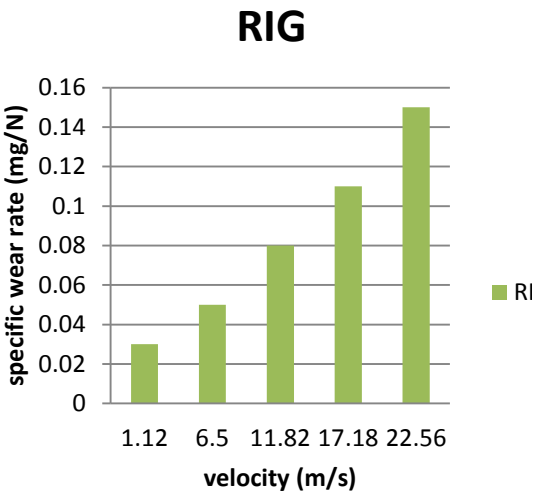

Figure 12 Extracted data for specific wear rate vs. velocity for RIG

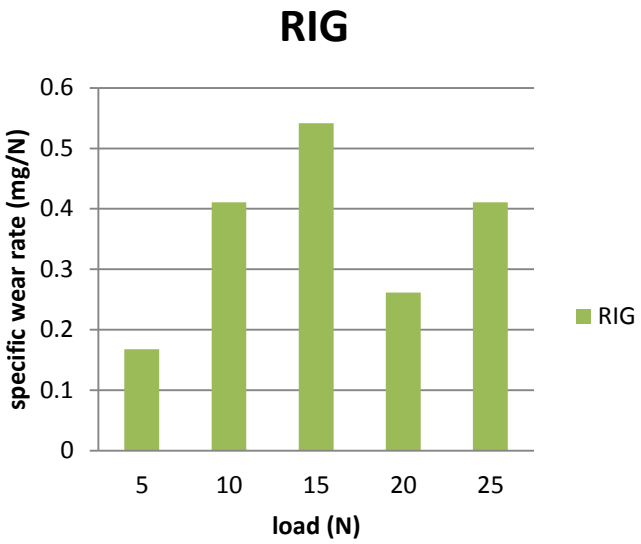

Figure 14 Extracted data for specific wear rate vs. load for RIG

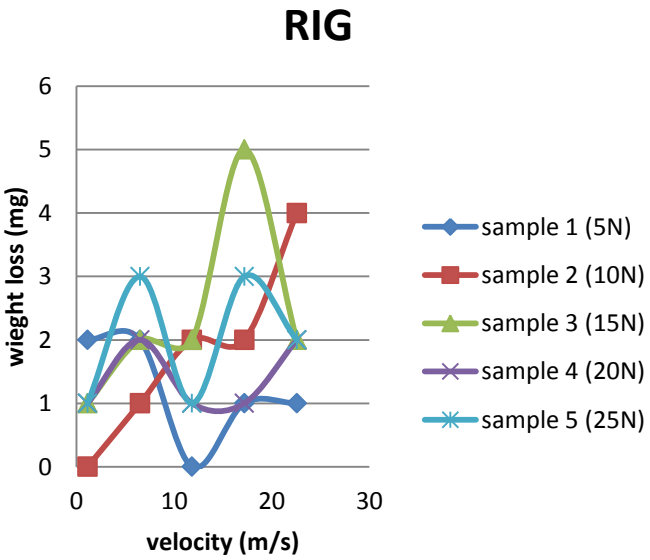

Figure 13 Effect of weight loss vs. velocity for RIG at different loads

For wear test using RIG, the duration of tribology test is constant which is within 20 minutes and was carried out under dry contact condition. The remaining debris after each test was removed before begins the new test using brush. The wear occur in this test is abrasion because RIG is smooth part, rubbing the hard part (stainless steel).

Fig. 11 gave inconstant pattern, but if it's looked in to detail, it showed for slow velocity (1.12 – 6.50 m/s), it result in lower weight loss at low load (5-10 N), and for other patterns, at higher velocity (11.82 – 22.56 m/s), higher weight loss were observed at lighter load (5-10 N).

While Fig. 12 gave increasing pattern in specific wear rate with increasing of velocity (1.12 – 22.56 m/s).

Fig. 13 shows the increasing pattern. The weight loss increase at lower velocity (1.12 – 6.50 m/s) then decrease at middle velocity (11.82 m/s) then increase again at higher velocity (17.18 – 22.56 m/s). Fig. 14 shows specific wear rate increase at load 5N -15N, slightly decrease at 20N and increase again at 25N.

Fluctuating value of weight loss suggest that adhesive bonding occur between RIG surfaces, the debris from the specimen wear will contact the RIG surfaces at certain points.

Effect of wear on RRHC

For RRHC, the specimen was also cut into 20x10x6 mm for wear tests. Ranges of velocity (1.12m/s – 22.56m/s) were carried out:

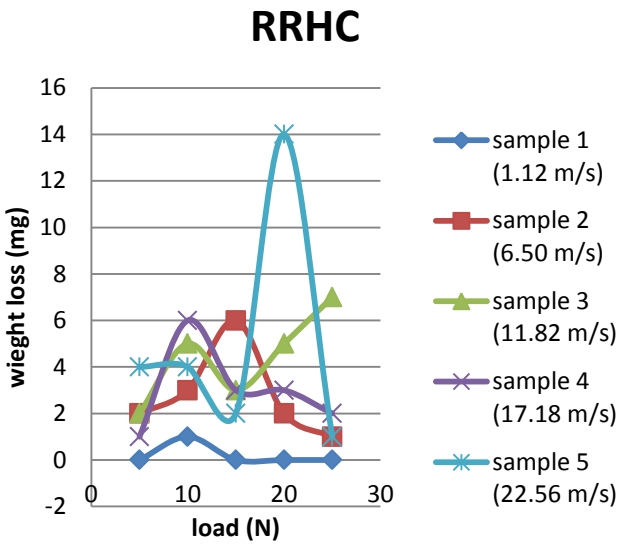

Figure 15 Effect of weight loss vs. load for RRHC for different velocity

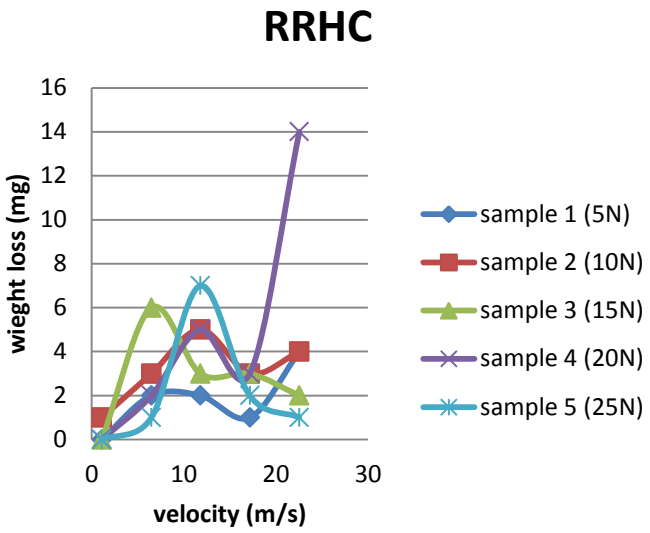

Figure 17 Effect of weight loss on velocity for RRHC at different load

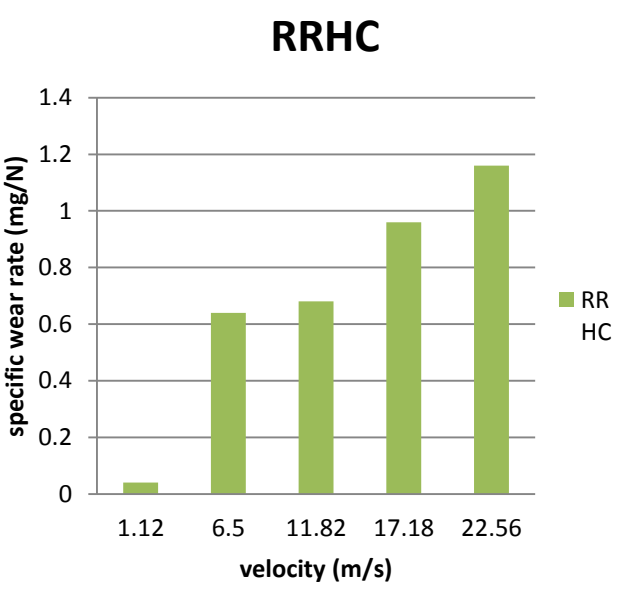

Figure 16 Effect of specific wear rate vs. velocity for RRHC

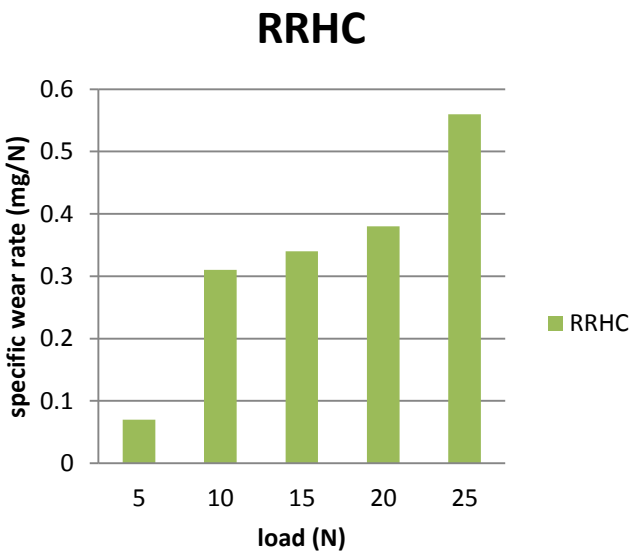

Figure 18 Effect of specific wear rate vs. load for RRHC

For wear test using RRHC, the duration of tribology test is constant which is within 11 minutes and was carried out under dry contact condition. The remaining debris after each test also was removed before begins the new test using brush. Similarly, the wear occurred in this test was abrasion because same condition as stated before, RRHC is smooth part, rubbing the hard part (stainless steel).

Figs. 15 and 16 show various patterns, at lowest velocity (1.12 m/s), the lowest weight loss at ranges of load (5-25N), but at higher velocity (6.50 – 22.56 m/s), the weight loss increasing with load applied increase. But at velocity of 22.56 m/s, the highest weight loss detected, its call catastrophic wear, it happen when RRHC material was go through abrasive wear until passing acceptable damage point.

Fig. 16 shows increasing pattern in specific wear rate with increasing of velocity (1.12m/s – 22.56m/s). In details, RRHC had lowest specific wear rate at lowest velocity (1.12m/s) then suddenly the specific wear rate increase at velocity of 6.50 m/s then increasing in uniform pattern for higher velocity (11.82m/s – 22.56m/s).

Figs.17 and 18 show at lower load (5N-10N), the weight loss increase at velocity of 1.12 m/s

until 11.82 m/s, slightly decrease at 17.18 m/s and then increase again at 22.56 m/s. For middle load (15N), the weight loss increase until velocity of 1.12 m/s, slightly decrease at velocity of 6.50 m/s until 22.56 m/s. For higher load (20N-25N), the weight loss increase at velocity 1.12 m/s up to 11.82 m/s, then for load of 20N, the weight loss just decrease with increasing velocity but for load of 25N, the weight loss just slightly decrease at velocity of 17.18 m/s, then the weight loss suddenly increase again at velocity of 22.56 m/s. These data was further simplified by extracting the data and comparing for both RIG and RRHC as shown in Figs.19 and 20.

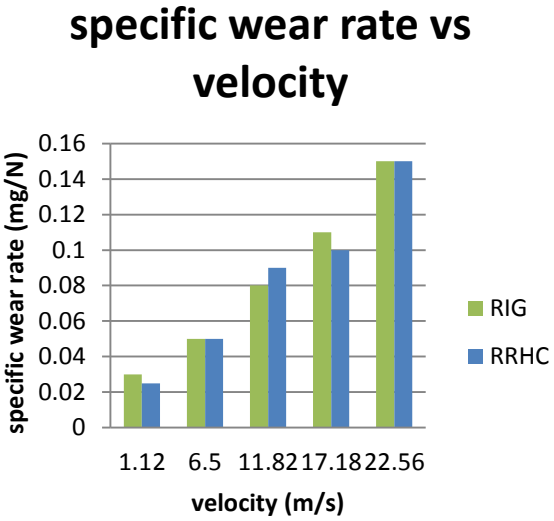

Figure 19 Extracted data specific wear rate vs. velocity for RIG and RRHC

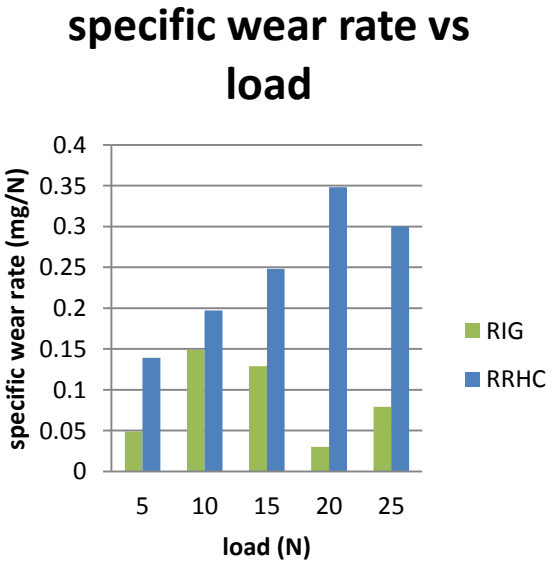

Figure 20 Extracted data for specific wear rate vs. load for RIG and RRHC

In comparison, for both specimens, RIG and RRHC, due to Fig. 19, specific wear rate versus velocity show almost same pattern, almost the same value of specific wear rate, as in Fig. 20, specific wear rate versus load show different pattern and value, highest specific wear rate for RIG material at load of 10N and highest specific wear rate for RRHC material at load of 20N. This result supported previous researcher (El-Tayeb and Nasir) that stated the wear are strongly depend upon the applied load.

From Fig. 20, RRHC had a worst wear resistance as compared to RIG because the graph of RRHC gave higher value of specific wear rate when increasing the applied load.

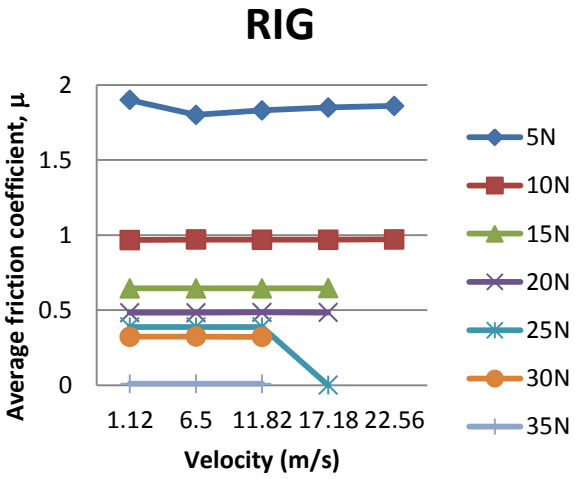

Figure 21 Average friction for RIG

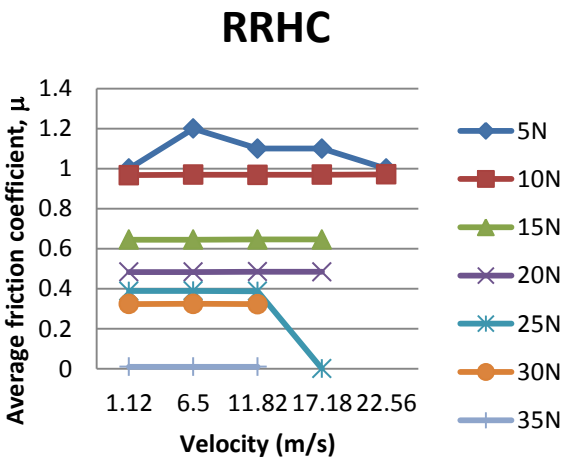

Figure 22 Average friction for RRHC

The average coefficient of friction (COF) was measured at different load and velocity. The COF was minimized until it reached the value at 0.01 for both RIG and RRHC at 35N and high velocity as shown by linear flat line for all samples, but PPHC catastrophic failure. This is as shown in Figs. 21 and 22 at different loads and velocities.

4. CONCLUSION

Compression result showed that the presence of gunny fibre as reinforcement resulting highest load i.e. more than 8N comparing to RRHC and PPHC which is less than 1N. The average maximum displacement is highest for RRHC at 1.8 cm while that for RIG and PPHC is at 1.6 and 0.9 cm respectively. RRHC does has some recovery ability after exceed maximum load applied to be sustained, but RIG does not has self-healing properties. The specific wear rate for RIG is lower than RRHC and PPHC at increasing load for approximately 0.35 mg/N and comparable at increasing velocity approximately 0.16 mg/N. The highest specific wear rate for RIG and RRHC is at 10N and 20N respectively indicating the wear endurance for load is better performed in RRHC compared to RIG and PPHC. Friction was minimized to 0.01 for both RIG and RRHC but PPHC catastrophic failure. Finally the worn surface morphology of both materials were studied using scanning electron microscope (SEM) in relation to external deformation. For future work, abrasion in certain lubricants and different environments are recommended.

ACKNOWLEDGEMENT

This work was supported by the Incentive Grant Universiti Sains Malaysia and Fundamental Research Grant Scheme [203/PMEKANIK/6071192] under Ministry of Education, Malaysia.

REFERENCES

Acilar M., Gul F. 2004. Effect of the applied load, sliding distance and oxidation on the dry sliding wear behavior of Al-10Si/SiC composite produced by vacuum infiltration technique, Material and design 25, 209-217.

El-Tayeb N.S.M and Mostafa I.M, 1996. The effect of laminate orientations on friction and wear mechanisms of glass reinforced polyester composite, Wear 195, 186-191

Godfrey D., 1995. Friction oscillation with a pin-on-disk tribometer, Tribology International 28 (2), 119-126.

Guicciardi S., Melandri C., Lucchini F. and Portu G. D. 2002. On data dispersion in pin-on-disk wear test, Wear 252, 1001-1006.

Harsha A.P., Tewari U.S. and Venkatraman B. 2003. Three-body abrasive wear behaviour of polyaryletherketone composites, Wear 254, 680-692.

Holmberg K. and Wickstrom G., 1987. Friction and wear test of polymers. Wear 115, 95-105.

Nair R.P., Griffin D., Randall N.X. 2009. The use of pin-on-disk tribologi test method to study three technique industrial applications, Wear 267, 823-827.

Nasir R.Md. and Azizan M. M. 2011. Adhesion and Friction E-Glass Fibre Reinforced Epoxy Composites for Tribo-Applications, Journal of Thermoplastic Composites, JTC 404461, Accepted

Quintelier J., Samyn P., Baests P. D., Doncker L.D., Hemelrijck D.V. and Sol H., 2006. Influence of re-adhesion on the wear and friction of glass fibre-reinforced polyester composites, the journal adhesion 82, 1033-1060.

Quintelier J., Baets P.D, Samyn P. and Vhemelrijick D. 2006. On the SEM features of glass-polyester composite system subjected to dry sliding wears. Wear 261, 703-714.

Rahman M.R., Huque M.M., Islam M.N., Hasan M., 2008. Improvement of physio-mechanical properties of jute fiber reinforced polypropylene by post-treatment, Composite, 1739-1747.

Unal H., Sen U. and Mimaroglu A., 2004. Dry sliding wear characteristics of some industrial polymers against steel counterface, Tribology International 37, 727-732.

Yoon E.S., Kong H., Kwon O.K., Oh J.E. 1997. Evaluation of frictional characteristics for pin-on-disk apparatus with different dynamic parameter. Wear 203-204, 341-349.

Yousif B.F., Lau S.T.W., McWilliam S. 2010. Polyester composite based on betelnut fibre for tribological applications, Tribology International 43, 503-511.

Paper Reference ID: RTC 042

INVESTIGATION ON THE EFFECT OF CRUDE PALM OIL (CPO) ON THE SURFACE ROUGHNESS AND TOOL WEAR IN TURNING SS304

N. N. Md Ibrahim*, M. Bin Sudin and F. Mohd Nor

Department of Mechanical Engineering
Universiti Teknologi PETRONAS
31750 Tronoh, Perak, Malaysia.
E-mail: nor.nurulhuda7479@gmail.com

ABSTRACT

Cutting fluid is considered as an essential component in the metal cutting operation. The need for renewable and biodegradable cutting fluids is increasing due to stronger environmental concerns and growing regulations over contamination and pollution. Over the years, many researches on vegetables oil have been conducted because vegetable oils are one of the promising sources with respect to their renewability and environmentally favorable oils. In this research, the turning tests were conducted at four different machining speeds (500,710, 1000 and 1400 rpm) while the depth of cut and feed were kept constant at 0.5 mm and 0.23 mm/rev, respectively utilizing Solkut 2140 and CPO as the cutting fluids. The results indicated in general, CPO outperformed Solkut 2140 by improving the surface finish and reducing the tool wear. CPO has been used as a cutting fluid in this work because it provides the desirable quality for boundary lubrication, biodegradable, less toxic and easily obtained sources which comes in economical price.

Keywords: CPO, surface roughness, tool wear, turning

1. INTRODUCTION

Stainless steels are known for their resistance to corrosion but their machinability is more difficult than the other alloy steels due to reasons such as having low heat conductivity, high built-up edge (BUE) tendency and high deformation hardening (Kopac and Sali, 2001). The difficulty of machining austenitic stainless steels was also reported by Akasawa et al. (2003). Problems such as poor surface finish and high tool wear are common in machining of austenitic stainless steels (Kosa and Ney, 1989). Work hardening is recognized to be responsible for the poor machinability of austenitic stainless (Jiang et al., 1997). In addition, they bond very strongly to the cutting tool during cutting operation and when chip is broken away, it may bring with it a fragment of the tool, particularly when cutting with cemented carbide tools. Therefore, cutting fluids have been introduced to lessen some of these problems encountered during the machining operation.

**Corresponding author*

1.1 Cutting Fluids

Cutting fluids have been introduced into the cutting process with the purpose to improve the characteristics of the tribological processes which are always present on the contact surfaces between the tool and the workpiece. Oils, emulsions, semisynthetics and synthetics are four general types of cutting fluids that are commonly used in machining operations. The first study about cutting fluids had been determined by W.H. Northcott in 1868 with a book entitled "A Treaties on Lathes and Turning". In the middle of 1890's, F.W. Taylor emphasized that using cutting fluids would allow to employ higher cutting speeds resulting in higher material removal rates and at the same time, prolong the tool life (Cakir et al., 2007). It had been concluded that the application of cutting fluids in machining processes would make shaping process easier (DeGarmo et al., 2003 ; Schey, 2000).

Vast quantities of cutting fluids are used annually to accomplish a number of objectives for example to reduce friction and wear, to cool the cutting zone, to reduce power consumption, to aid in providing satisfactory chip formation, to flush away the chips from the cutting zone and to protect the machine surface from environmental corrosion. The good cutting fluids must possess good lubricating qualities, high thermal conductivity for cooling purpose, stable against oxidation, high flash point (should not entail fire hazard), has viscosity that will permit free flow from the workpiece and dripping from the chips and must not cause skin irritation or contamination (Kalpakjian and Schmid, 2006).

The use of conventional petroleum-based cutting fluids is potentially dangerous. This is because, they can cause environmental pollution due to chemical dissociation of the cutting fluid at high cutting temperature, biological issues mainly the dermatological problems to the machine operators, water pollution and soil contamination during disposal (Soković and Mijanović, 2001). Approximately, 40% of mineral oil-based lubricants are not properly disposed causing the environmental damage. Prolong

exposure to cutting fluids may cause skin irritation or skin cancer. The possibility also exists of a hazard to the lungs from the inhalation of mist at the working environment. These situations lead to the growing demand for biodegradable cutting fluids (Kipling, 1977).

The objective of this work is to study and to compare the performance of CPO to commercially available cutting fluid which is Solkut 2140 in terms of surface roughness produced and tool wear developed during turning operation by using coated carbide insert as cutting tool and AISI 304 austenitic stainless steel as workpiece material.

1.2 Vegetable-based Cutting Fluids

Over the years, vegetable oils and fats have been used and retained their importance as metalworking fluids. The use of vegetable oils in metalworking applications may lessen the biological problems faced by the machine operators. Vegetable oils have good lubricating ability and had been used for the formulation of metal cutting emulsions (Herdan, 1999). Fewer companies like Blazer (Swiss), Cargill Industrial Oils & Lubricants (USA) and Renewable Lubricants (USA) are working towards commercializing vegetable oil based cutting fluids. Yamanaka et al. (2000) conducted the research on vegetable-based metal working lubricant additives namely fatty acids on the grinding performance using various types of carboxylic acids. The fatty acids formulations have shown the best grinding performance for all oiliness agents, friction modifier and as extreme pressure agents. Chiffre and Belluco (2002) studied the performance of cutting fluids for turning, drilling, reaming and tapping operation for austenitic stainless steel and other four materials. Water-based and straight oils, including mineral, synthetic and vegetable-based formulations were tested. The results, on austenitic steel, revealed that the cutting forces developed under vegetable oils and esters modes were low compared to reference mineral oils. However, the tool life was escalated under vegetable oils/ester modes lubrication.

Carcel et al. (2005) evaluated sunflower oil, corn oil, soyabean, olive oil from press extraction and solvent extract ion under the boundary lubrication condition for stamping operation. All the vegetable oils coated on three types of sheet exhibited low values of friction during stamping operation when compared to the reference mineral oil. They claimed that among all the oils, the best results were obtained with olive oil. Surface topography results indicated that, lubrication performance under vegetable oils for steel sheets is better than mineral oil. Raynor et al. (2005) formulated five metal working fluids (MWFs) emulsions from soyabean oil. The results were compared with those obtained under commercial MWFs emulsions formulated using vegetable oil and oil made from mineral oil. It was reported that, under impaction mechanism, both the experimental fluids and commercial fluids generated similar amount of mist. In addition, air-oxidised soyabean produced less mist under impaction and centrifugal mechanisms compared to petroleum-based fluid. They concluded that the air-oxidised soyabean oil is the most promising candidate among the experimental fluids. Lovell et al. (2006) utilized a blend of canola oil and boric acid as forming lubricant for the deep drawing operation. It was reported that the boric acid and canola oil combination had a steady state friction value and it was 44% less than the commercial fluid case. Likewise, the new blended lubrications produced better surface finish compared to the commercial fluid. The findings concluded that the canola oil and boric acid combination increases the formability of steel sheets.

The development and application of methodologies for the formulation of sustainable neat-oil (immiscible with water) metal removal fluids were studied by Abdalla et al. (2007). Vegetable-based oils such as coconut, sunflower, rapeseed, palm olive and rapeseed (high erucic) were selected for the study. Tribological studies revealed that very low friction values were found under naturally derived cutting oil compared to commercial oil. From micro tap test, it was reported that the vegetable oil with naturally derived additives produced low cutting force and torque while machining on stainless steel metal. Finally, it was concluded that naturally derived oils were better for stainless steel machining. The influence of coconut oil as a cutting fluid on tool wear and surface roughness during turning of SS304 had been studied by Xavier and Adithan (2009). The performances of coconut oil were compared with another two cutting fluids namely an emulsion and a neat cutting oil. From the results, it was found out that for any combination of cutting parameters, coconut oil always outperformed the other two cutting fluids.

1.3 Palm Oil

Palm oil is edible plant oil derived from the fruit of the oil palm (*Arecaceae Elaeis*). Palm oil is an important component for making soap, washing powders, personal care products, for treating wounds and has controversially found a new use as a feedstock for biofuel (Choo and Lau, 2009). Palm oil has potential application as lubricant in rolling process mainly in steel industry (Shashidara and Jayaram, 2009).

Malaysia currently accounts for 39% of world palm oil production and 44% of world exports. This subsequently makes Malaysia accounts for 12% and 27% of the world's total production and exports of oils and fats, respectively (Malaysian Palm Oil Industry, 2011). Due to the abundant sources of palm oil, the research was conducted to explore the potentiality of CPO as a cutting fluid in the machining operation such as the turning process. The vast sources of palm oil in Malaysia make it easily available and economically attractive choice. The properties of CPO are shown in Table 1 (Nurul Qurratu'aini Nordin, 2009).

Table 1 Properties of crude palm oil

State	Liquid
Colour	Reddish yellow
Viscosity	64.69 cSt at 40^{o}C
Viscosity index	95
pH	4.8
Flash point	116^{o}C
Relative density	0.9
Melting point	30^{o}C
Solubility	Insoluble in water, soluble in hydrocarbon

Palm oil contains palmitic acid which is in saturated form. This saturated fatty acid forms triglycerides which provide desirable qualities for boundary lubrication due to their long and polar fatty acid chains. These chemical structures provide high strength lubricant films that interact strongly with metallic surface, subsequently reducing friction and wear (Siniawski et al., 2007). The polarity of fatty acids produces oriented molecular films which provide oiliness and impart antiwear properties. Fatty acids are thus believed to be key substances with regard to lubricity (Havet et al., 2001). Besides its lubricity and abundant sources, palm oil offers other significant benefit such as having less toxicity. It other words, it can be disposed without causing so much harm to the machine operators and/or the environment.

2. METHODOLOGY

The experiment was carried out by using conventional lathe machine. The machining tests were performed by single point continuous turning on Excel Machine Tool XL 510 heavy duty lathe. AISI 304 grade austenitic stainless steels with average hardness of 70 HRB in cylindrical form were used as workpiece material. Titanium Nitride (TiN) with Cobalt-Nickel inserts produced by Korloy Inc. with ISO code CNMG 120408 were used as the cutting tool. The insert was clamped mechanically on a rigid tool holder WIDAX's PCLNR 2525 M12. As far as possible, the tests were carried out in accordance with ISO 3685. The cutting fluids used were CPO (straight oil extracted from palm oil) and Solkut 2140. Solkut 2140 was diluted in water to the ratio of 1:10 to form an emulsion. The portion of water used is 10 and the cutting fluid is 1.The tests were conducted at four different machining speeds. They were 500 rpm, 710 rpm, 1000 rpm and 1400 rpm. The experiments were repeated several times at each machining speed to obtain more data for accuracy and consintency. The depth of cut and feed were fixed, 0.5 mm and 0.23 mm/rev, respectively. The machining speeds, depth of cut and feed were chosen by taking into consideration the cutting tool manufacturer's recommendations and industrially used values for these materials. The workpiece was clamped rigidly between the chuck and tailstock to reduce vibration during turning operation. The cutting fluids were delivered externally with 450 ml/min to the cutting zone along an approximately overhead direction through a single nozzle. Figure 1 shows the experimental set up for turning operation.

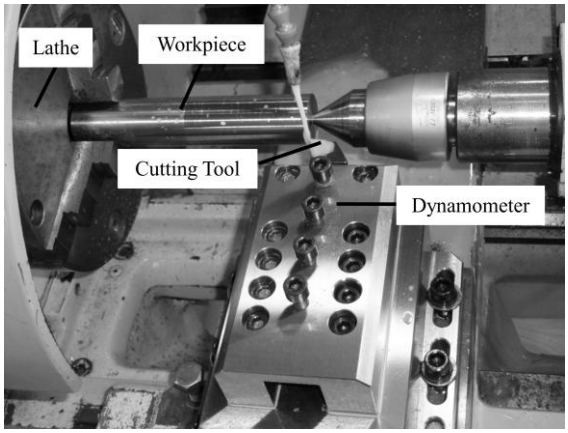

Figure 1 The experimental set up for turning operation.

After the machining process, the insert was removed and the average surface roughness (R_a) of the workpiece was measured using MAHR's Perthometer Concept PGK 120 measuring instrument and Mitutoyo SURRTEST SV-3000. Tool wear progression was observed and measured using Mitutoyo Quick Vision Pro 202 3D noncontact measuring equipment with 64x magnification. The tool wear progression was recorded at 10 minutes interval from 0 to 40 minutes. The average values of surface roughness and tool wear were used in the analysis.

3. RESULTS AND DISCUSSIONS

3.1 Surface Roughness

Surface finish influences not only the dimensional accuracy of the machined parts but also their properties and their performance in service. The R_a obtained in the range of 0.24 µm to 1.74 µm. The average values of these measurements are plotted in Figure 2. Figure 2 shows that, machining by utilizing CPO as the cutting fluid produced lower R_a compared to Solkut 2140.

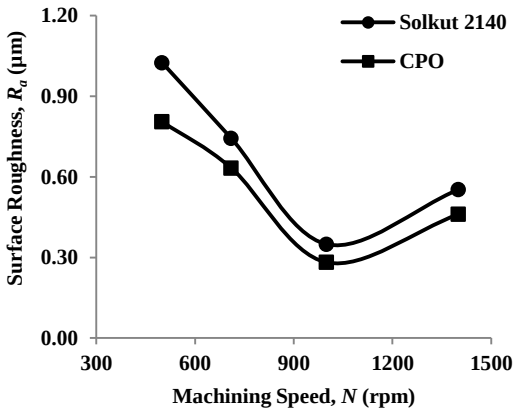

Figure 2 Variation of surface roughness with cutting fluid and machining speed.

The general trend in the curves in Figure 2 is that, when machining speed is increased, R_a decrease until a minimum value is reached. Beyond 1000 rpm, R_a increase. The highest R_a observed at the lowest machining speed (500 rpm) due to formation of BUE which is shown in Figure 3. The presence of BUE on the tool tip leads to poorer surface finish. BUE and chipping are closely associated with each other in the case of machining ductile materials which in this case, it is SS304. Both of them lead to the increase of R_a. At lower machining speed, BUE becomes stronger than that were formed at higher machining speed. Thus, affecting the surface finish of the turned parts. The decrease in R_a with increasing machining speed up to 1000 rpm can be explained by decreasing BUE formation tendency. At higher machining speed (1000 rpm), cutting zone temperature increases and this, in turn, softens and decreases the strength of BUE. Therefore, a lower adhesion force was observed between the BUE and cutting tool at higher machining speed. This induces less adhesive force on the cutting edge and thus less chipping of cutting tool was observed due to the detachment of BUE during cutting. However, further increase in machining speed caused an increase in R_a. This can be attributed to the increasing of cutting tool nose wear at 1400 rpm, which is the highest machining speed employed. At this machining speed also, the temperature of the cutting zone increases to a level at which cutting edge losses its strength which resulted in chipping occurrence (Ciftci, 2006).

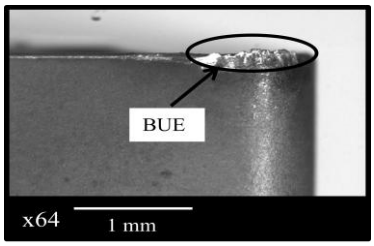

Figure 3 BUE formations at 500 rpm using Solkut 2140 as cutting fluid.

In this research, CPO produced better surface finish due to fatty acid content in it. It has been explained in earlier section that the fatty acid forms triglycerides which provide desirable qualities for boundary lubrication due to their long and polar fatty acid chains. Free fatty acids are suggested to act as boundary additives, by formation of protective complexes of the acid with the metal surfaces. Fatty acids react with the surface to form a protective layer. The strength of this protective film depends heavily on the strength of the interactions between the molecules making up the film. Slimmer molecules allow closer packing, increasing the intermolecular interactions and providing a stronger film (Fox et al., 2004). Thus, fatty acids are believed to be key substances with regard to lubricity. In Solkut 2140 case, this cutting fluid acted more towards cooling the cutting zone rather than lubricating the cutting area. This is due to the high portion of water used to dilute Solkut 2140 which is 10 to 1 to form an emulsion. Therefore, it is hard to say that Solkut 2140 has good lubricating ability since the main purpose of this emulsion is to act as a coolant to reduce the temperature at the cutting zone during turning operation.

3.2 Tool Wear

According to standard ISO 3685, the time at which the tool ceases to produce a workpiece of desired size and surface quality usually determines the end of useful tool life. Tool wear generally classified as flank wear, crater wear, nose wear, notching, chipping and gross fracture. Flank wear occurs on the relief (flank) face of the tool. Generally, it is attributed to rubbing of the tool along the machined surface, causing adhesive/or abrasive wear and high temperatures, which adversely affect tool material properties. Figure 4 shows flank wear produced after 40 minutes of machining for both Solkut 2140 and CPO at 710 rpm.

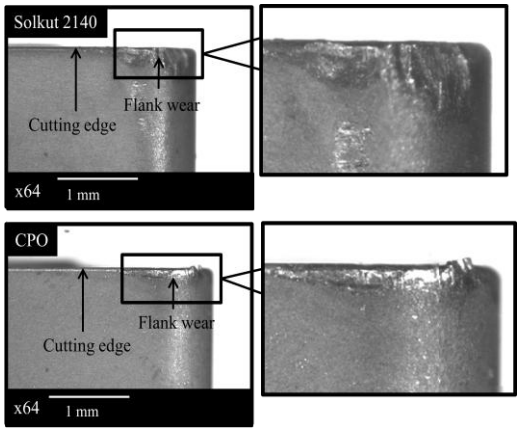

Figure 4 Flank wear formation at 710 rpm after 40 minutes of machining.

Figure 5 shows the plotted average values of flank wear (V_b) produced by utilizing Solkut 2140 and CPO after 40 minutes at different machining speed. CPO produced smaller flank wear compared to when turning utilizing Solkut 2140 as the cutting fluid. It is also seen from Figure 5 that the machining speed has significant influence on the tool wear developed. From Figure 5, at the lowest machining speed, it produced the highest V_b. By further increasing the machining speed to 1000 rpm, V_b decreased and beyond that, V_b increased. Poor performance of the tool at lower machining speed can be explained by the influence of the heat on the cutting tool. This is because in metal cutting, it involves large amount of heat generation and in case of SS304 machining, the heat does not dissipate rapidly due to low thermal conductivity of this material. At the lowest machining speed, the temperature of steel chips that formed at this machining speed was affected most from the heat. Therefore, the chips that were produced at this machining speed have the highest temperature compared to those chips that were produced at higher

machining speeds. Lower machining speed also leads to increasing of contact time on the rake face as the chips moved slowly when compared to higher machining speeds that were employed. In view of these findings, the high chip temperature and the long contact time on the rake face gave rise to thermal softening of the tool by conduction of the heat from the chips to the tool. This, in turn, reduces wear resistance of the tool (Korkut et al., 2004).

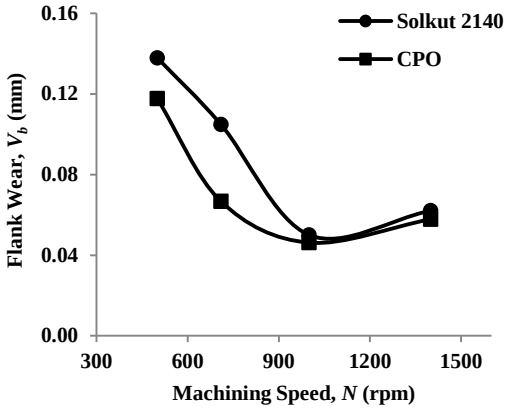

Figure 5 Flank wear at different machining speeds after 40 minutes of turning operation.

Besides flank wear, crater wear was also observed on the cutting tool after the turning operation. When chip flows across the rake face, severe friction between the chip and rake face developed. This leaves a scar on the rake face which usually parallels to the major cutting edge which is known as crater wear and the examples are shown in Figure 6. From Figure 6, the crater wear produced by utilizing CPO as cutting fluid is smaller compared to Solkut 2140. The presence of this wear changes the tool-chip interface contact geometry. CPO produced slightly better result again due to the desirable quality that CPO possesses which is providing the boundary lubrication during turning operation.

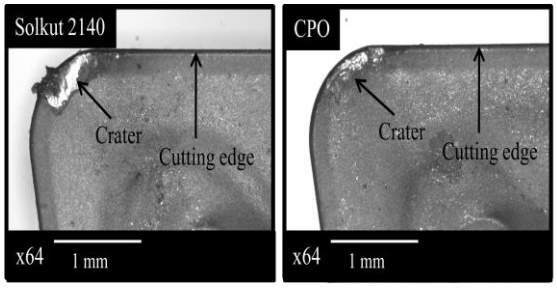

Figure 6 Crater wear formation at 500 rpm after 40 minutes of machining.

Figure 7 shows the pattern of crater wear produced by utilizing Solkut 2140 and CPO after 40 minutes at different machining speed. The trend is quite similar to flank wear's trend since the factors influencing flank wear also influence crater wear. The most significant factors influencing crater wear are temperature at the tool-chip interface and the chemical affinity between the tool and the workpiece materials. Their values are almost twice of the flank wear developed. At the lowest machining speed, high temperature and long contact time gave rise to thermal softening of the tool by conduction of the heat from the chips to the tool. Thus, resulting in lower wear resistance of the tool during turning operation which in turn, increased the wear rate of the cutting tool. Generally, crater wear is attributed to diffusion mechanism which is the movement of atoms across the tool-chip interface. Since the diffusion rate increases with increasing temperature, craters wear increases as the temperature at the cutting zone increase. This applies to the lowest machining employed by having long contact time leading to temperature rise on the cutting zone.

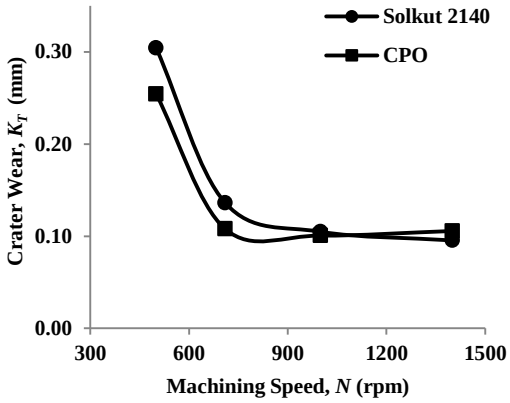

Figure 7 Crater wear at different machining speeds after 40 minutes of turning operation.

4. CONCLUSIONS

Experiments involving coated carbide tool inserts and SS304 as work material under varying machining speeds utilizing Solkut 2140 and CPO as cutting fluids were performed. The cutting fluids' effectiveness in improving the surface finish and reducing the tool wear was found by comparing their relative performance. Machining speed was found to have a significant effect on the surface finish of the turned parts and tool wear developed. With increasing machining speed until 1000 rpm, R_a decreased and beyond that, R_a increased. Higher R_a at lower machining speeds are attributed to high BUE formation tendency. The trends were quite similar for tool wear developed. Flank wear and crater wear are dominant wear that were observed on the cutting tool. The poor performance of the cutting tool at lower machining speeds could well be explained by the thermal softening of the tool due to the higher influence of the heat on the cutting tool and less efficiency of heat dissipation. From the test results, CPO was found as good as commercially available cutting fluid which is Solkut 2140. CPO was found to be promising alternative for mineral based oils due to its good quality for boundary lubrication, abundance sources and biodegradability.

ACKNOWLEDGEMENT

The author wish to thank the technologists for providing help and support during the experiments. Many thanks to Universiti Teknologi PETRONAS Postgraduate Department for financing the research materials. The author also would like to thank Felcra Nasarudin which is located in Bota, Perak Tengah for providing the crude palm oil for research purpose.

REFERENCES

Abdalla, H.S., Baines, W., McIntyre, G. and Slade, C. 2007. Development of novel sustainable neat-oil metal working fluids for stainless steel and titanium alloy machining, Part I - Formulation development, Journal of Advanced Manufacturing Technology, 34: 21-33.

Akasawa, T., Sakurai, H., Nakamura, M., Tanaka, T. and Takano, K. 2003. Effect of free-cutting additives on the machinability of austenitic stainless steel, Journal of Material and Processing Technology, 143-144: 66-71.

Cakir, O., Yardimeden, A., Ozben, T. and Kilickap, E. 2007. Selection of cutting fluids in machining processes, Journal of Achievements in Materials and Manufacturing Engineering, 25(2): 99-102.

Carcel, A.C., Palomares, D., Rodilla, E. and Pérez, M.A. 2005. Evaluation of vegetable oils as pre-lube oils for stamping, Material Design, 26: 587-593.

Choo, Y.M. and Lau, L.N. 2009. Palm oil as feedstock for biodiesel: Production and export from Malaysia, IEA Bioenergy Task 40/ERIA Workshop, AIST, Tsukuba, Japan.

Ciftci, I. 2006. Machining of austenitic stainless steel using CVD multi-layer coated cemented carbide tools, Tribology International, 39: 565-569.

De Chifre, L. and Belluco, W. 2002. Investigations of cutting fluid performance using different machining operations, Lubrication Engineering, 18-25.

DeGarmo, E.P., Black, J.T. and Kosher, R. A. 2003. Materials and processes in manufacturing, ninth ed., John Wiley and Sons, Inc., United States.

Fox, N.J., Tyrer, B. and Stachowiak, G.W. 2004. Boundary lubrication performance of free fatty acids in sunflower oil, Tribology Letters, 16: 275-281.

Havet, L., Blouet, J., Valloire, R., Brasseur, E. and Slomka, D. 2001. Tribological characteristics of some environmentally friendly lubricants, Wear, 248: 140-146.

Herdan, J.M. 1999. Rolling fluids based on vegetables oils, Journal of Synthetic Lubrication, 16: 201-210.

Jiang, L., Roos, A. and Liu, P. 1997. The influence of austenite grain size and its distribution on chip deformation and tool life during machining of AISI 304L, Metallurgical and Materials Transactions, 28A: 2415-2422.

Kalpakjian, S. and Schmid, S. 2006. Manufacturing engineering and technology, fifth ed., Pearson Prentice Hall, Singapore.

Kipling, M.D. 1977. Health hazard from cutting fluids, Tribology International.

Kopac, J. and Sali, S. 2001. Tool wear monitoring during the turning process, Journal of Material Processing Technology, 113: 312-316.

Korkut, I., Kasap, M., Ciftci, I. and Seker, U. 2004. Determination of optimum cutting parameters during machining of AISI 304 austenitic stainless steel, Materials and Design, 25: 303-305.

Kosa. T. and Ney, R.P., Sr. 1989. Machining of stainless steels: Metals handbook, ninth ed., ASM International.

Lovell, M., Higgs, C.F., Deshmukh, P. and Mobley, A. 2006. Increasing formability in sheet metal stamping operations using environmentally friendly lubricants, Journal of Material Processing Technology, 177: 87-90.

Malaysian Palm Oil Industry, http://www.mpoc.org.my/Malaysian_Palm_Oil_Industry.aspx, access on 30 August 2011.

Nurul Qurratu'aini Nordin, 2009. The Study into the potential of using palm oil as a cutting fluid in the machining operations, B.E Thesis, Universiti Teknologi PETRONAS, Malaysia.

Raynor, P.C., Kim, S.W. and Bhattacharya, M. 2005. Mist generation from metal working fluids formulated using vegetable oils, Annals of Occupational Hygiene, British Occupational Hygiene Society, 40: 283-293.

Schey. J.A. 2000. Introduction to manufacturing processes, third ed., McGrawHill International, Singapore.

Shashidara, Y.M. and Jayaram, S.R. 2009. Vegetable oil as a potential cutting fluid - An evolution, Tribolology International.

Siniawski, M.T., Saniei, N., Adhikari, B. and Doezema, L.A. 2007. Influence of fatty acid composition on the tribological performance of the two vegetable-based lubricants, Journal of Synthetic Lubrication, 24: 101-110.

Soković, M. and Mijanović, K. 2001. Ecological aspects of the cutting fluids and its influence on quantifiable parameters of the cutting process, Journal of Material Processing Technology, 109: 181-189.

Xavior, M.A. and Adithan, M. 2009. Determining the influence of cutting fluids on tool wear and surface roughness during turning of AISI 304 austenitic stainless steel, Journal of Material Processing Technology, 209: 900-909.

Yamanaka, Y., Oi, T., Nanao, H. and Satoh, M. 2000. Development of new grinding fluids for CBN grinding wheel: Part V - A study on the grinding performance of various types of carboxylic acids, STLE Transactions, 56: 25-31.

Paper Reference ID: RTC 067

TAGUCHI METHOD FOR OPTIMISING THE MANUFACTURING PARAMETERS OF FRICTION MATERIALS

A.M. Zaharudin[1], R.J. Talib[2], M.N. Berhan[3], S. Budin[1] and M.S. Aziurah[1]

[1]Faculty of Mechanical Engineering, Universiti Teknologi MARA
13500 Permatang Pauh, Penang, Malaysia
E-mail: aznifa@ppinang.uitm.edu.my
[2]Advanced Materials Research Centre, SIRIM Bhd.,
Lot 34, Jalan Hi Tech 2/3, Kulim Hi Tech Park,
09000 Kulim, Kedah, Malaysia
E-mail: talibria@sirim.my
[3]Faculty of Mechanical Engineering, Universiti Teknologi MARA
40450 Shah Alam, Selangor, Malaysia
E-mail: berhan@salam.uitm.edu.my

ABSTRACT

Semi-metallic friction materials were produced by powder metallurgy method. This study investigated the optimization of manufacturing parameters (molding pressure, molding temperature and molding time) for friction materials using Taguchi Method. Physical properties (hardness and specific gravity) and tribological properties (wear and fade) were selected as the quality target. It was determined that molding pressure has the strongest effect on physical and tribological properties. It was observed that friction materials with optimal level of parameters proved to be the best performance in tribological behavior. Physical properties however, did not show any correlation with tribological properties.

***Keywords**:* Taguchi method, Tribological behavior, Friction material

1. INTRODUCTION

Brake friction material is a heterogeneous material that diverse in physical, mechanical and chemical properties of the developed formulation. They are classified as binders, reinforcements, fillers, friction modifiers. Friction and wear characteristics of the developed formulation cannot be predicted based on physical and mechanical properties. Selection of ingredient materials is the difficult task as it requires a great number of experiments to obtain reliable brake performance. A variety of techniques have been employed to investigate the development of ingredients for friction materials in order to provide stable friction, durability, adequate wear resistance, thermal conductivity and vibration for all braking, and acceptable environmental conditions (Cho et al., 2005; Jang et al., 2001; Tang and Lu, 2003).

Limited reports are available in the literature on the investigation on the manufacturing processes of brake friction materials even though they are critical for the tribological as well as physical properties of the brake friction materials. Ibhadode and Dagwa, 2008 in their study have demonstrated the relationship between the manufacturing parameters and tribological properties. In the automotive brake friction industry, friction material is manufactured using powder metallurgy according to two critical methods; first, hot molding of a mixture under high pressure and second, subsequent heat treatment (post-curing). The molding processes involves rearrangement of powder particles, the elastic deformation of the particles and finally, plastic deformation accompanied by reduction in porosity (Al-Qureshi et al., 2008). Heat treatment is performed to enhance curing uniformity and to relieve the residual stresses in the brake friction materials. Phenolic resin used as a binder in brake friction materials plays a crucial role in determining the tribological properties since the manufacturing conditions are affected by thermal properties of the binder (Bijwe et al., 2005; Kim et al., 2008). Hence in this work, the economical and viable experimental strategy based on Taguchi's parameter design has been used to analyze the effect of various manufacturing parameters of friction materials for molding in order to improve tribological properties.

Table 1: Ingredient of friction materials

Ingredients	wt.%	Ingredients	wt.%
Steel fiber	20	Iron oxide	8
Ceramic Fiber	10	Magnesium oxide	3
Friction dust	8	Copper chip	10
Iron powder	5	Barium sulphate	5
Phenolic resin	12	Calcium carbonate	4
Rubber	3	Graphite	12

2. METHODOLOGY

2.1 Sample Preparation

Friction material used in this work containing 12 ingredients is listed in Table 1. The friction material was prepared by mixing, pre-forming hot molding and post curing. Mixing was carried out in a turbula mixer for 30 min. The mixer could move in three dimensions during mixing process. The mixture was pre-formed under 20 tonnes of pressure for 3 min at room temperature. The mixture was molded by a hot press according to 8 different combinations of manufacturing parameters to form L8 (2^3) orthogonal array (OA) of the Taguchi. Post curing was then carried out in an oven at 120^{o}C for 60 min, 150^{o}C for 60 min and 180^{o}C for 120 min to relieve the residual stress in the friction material specimens. The surfaces of the friction material specimens were then grinded to attain the desired thickness and smooth surface.

Thermogravimeric analysis was carried out to obtain the transition temperature of phenolic resin. Figure 1 shows the DTG curve of phenolic resin indicating an exothermic reaction in temperature range between 140^{o}C to 170^{o}C.

Table 2: The experimental layout of Taguchi L8 orthogonal array

Set	A	B	C
1	1	1	1
2	1	1	2
3	1	2	1
4	1	2	2
5	2	1	1
6	2	1	2
7	2	2	1
8	2	2	2

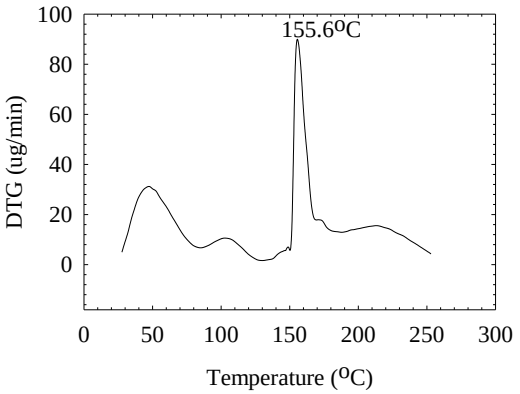

Figure 1 DTG analysis of phenolic resin as a function of temperature

A total of 8 experiments were designed according to standard Taguchi's L8 OA, which has 8 rows corresponding to the number of tests with three factors at two levels, as shown in Table 2. Molding pressure, molding temperature and molding time were selected as the manufacturing parameters to analyze their effect on the physical and tribological properties of the friction materials. The first column in Table 2 was assigned to molding pressure (A), the second to molding temperature (B) and the third to molding time (C). The settings of molding pressure (A) include 50 tonnes (level 1) and 60 tonnes (level 2); molding temperature (B) include 150^{o}C (level 2) and 170^{o}C (level 2); molding time (C) is set at 300 second (level 1) and 600 seconds level 3).

Four quality objectives of friction materials specimens are chosen, including hardness, specific gravity, wear and fade. Typically, large value of physical properties (hardness, *h* and specific gravity, *sg*) and small values of tribological properties (wear, *W* and fade, *f*) are desirable for the manufacturing operation. The experimental results are then transformed into a signal to noise (S/N) ratio. Taguchi proposes the use of the S/N ratio to measure quality characteristics deviating from the desired values. There are three categories of quality characteristic (output performance) in the analysis of the S/N ratio, i.e. larger-the better, nominal-the-best and smaller-the-better. The S/N ration for each level of process parameters is computed based on the S/N analysis. In spite of the category of the quality characteristic, process parameter setting with the highest S/N ratio corresponds to better quality characteristics. Therefore, the optimum level of the process parameters is the level with the highest S/N ratio with minimum variance. Statistical analysis of variance (ANOVA) is performed to observe the most significant

controlled factor for the manufacturing operations. Based on the S/N ratio and ANOVA analyses, the optimum combination of process parameters can be predicted. A confirmation run is conducted to verify the optimal process parameters obtained from the design parameter.

2.2 Measurement of Physical Properties

Surface hardness of the friction material specimen was measured using a Rockwell hardness tester (Mitaka TH300) in S scale. Specific gravity or density was measured using specific gravity meter (Shimadzu). The hardness and specific gravity test followed the standard test procedures MS 474: PART 2:2003 and MS 474: PART 1: 2003 respectively, develop by International Standard Organization, Malaysia Standard Department.

2.3 Measurement of Friction Performance

The friction and wear tests were performed using Chase dynamometer in accordance with SAE-J661. The specimens were cut to a dimension of 25 x 25 x 7 mm and then attached to the brake mechanism on brake drum. In this test, each specimen was pressed against a rotating brake drum with a constant speed of 417 rpm under the load of 647 N and subjected to test sequence in Table 3.

Table 3: Friction and wear test program

Block	Temperature (^oC)	Remarks
Burnish	82 - 93	Continuous braking 20 minutes
Baseline I	93	Intermittent braking 10 s ON, 20 s OFF, 20 applications
Fade I	93 – 288	Continuous and heater ON
Recovery I	260 – 93	Continuous and cooling ON
Wear	193 -204	Intermittent braking 20 s ON, 10 s OFF, 100 applications
Fade II	93 – 343	Continuous and heater ON
Recovery II	316 – 93	Continuous and cooling ON
Baseline II	93	Intermittent braking 10 s ON, 20 s OFF, 20 applications

The wear was expressed as in term of thickness loss, $W = (t_o - t_1)/t_o$ x 100%, where t_o and t_1 are the average thickness loss of the specimen before and after chase, respectively. Brake fade, f was obtained by calculating the decrement of the friction coefficient after the highest friction coefficient during friction test.

3. RESULTS AND DISCUSSION

3.1 Physical Properties

The results of the physical properties (surface hardness and specific gravity) measurements of the friction materials are shown in Table 4. The average hardness of the friction material was 76.63 $\pm$ 2.63 in Rockwell hardness S scale and the average specific gravity was 2.25 $\pm$ 0.14 g/cm^3.

In this study optimization is achieved by using S/N ratio larger-the better quality characteristics. The largest hardness and specific gravity would indicate the ideal situation. Friction materials with high surface hardness may reduce wear rate which indicates poor life. At high molding pressure, the densities increases and the pores between brake friction materials were reduced. High specific gravity reduces the wear and improves the thermal conductivity of material (Esswein Junior et al., 2008; Kurt and Boz, 2005). For the larger-the-better characteristics, the S/N ratio calculated as follows:

$$S/N = -10\log\frac{1}{n}\left(\sum_{i=1}^{n}\frac{1}{y_i^2}\right) \qquad (1)$$

where n is number of observations in the L8 orthogonal array and y_i is the average of observed data.

Table 4: Experimental results and S/N ratio for physical properties results

Set	*h* (HRS)	S/N ratio (dB)	*sg* (g/cm^3)	S/N ratio (dB)
1	72	37.147	2.25	7.044
2	73	37.266	2.25	7.044
3	71	37.025	2.20	6.848
4	80	38.062	2.18	6.769
5	86	38.690	2.27	7.121
6	80	38.062	2.32	7.310
7	76	37.616	2.21	6.888
8	75	37.501	2.34	7.384

h: hardness; *sg*: specific gravity

Table 5: ANOVA table for surface hardness

Factor	Sum of squares	Contribution (%)	*p*- value
A	0.7016	31.45	0.148
B	0.1153	5.17	0.588
C	0.0213	0.96	0.818

Table 6: ANOVA table for specific gravity

Factor	Sum of squares	Contribution (%)	*p*- value
A	0.1244	37.68	0.105
B	0.0.493	14.93	0.344
C	0.0460	13.92	0.363

ANOVA is used to identify the relative importance of the manufacturing parameters affecting the quality characteristics. The ANOVA analysis for surface hardness and specific gravity are shown in Table 5 and Table 6, respectively. This analysis was carried out for significant level of α = 0.05, for confidence level of 95%. The order of the percentage contribution reflects the relative importance in each factor. The tables suggested that the factor A, molding pressure has the strongest effect on the surface hardness (Kim et al., 2003) and specific gravity, followed by molding temperature and finally molding time. However, all the factors have insignificant effect to surface hardness and specific gravity because their *p*-values are more than 0.05. Hardness and specific gravity test is used as quality control during production of friction materials.

3.2 Tribological Behavior

The eight friction materials developed by L8 OA exhibited the coefficient of friction in the range of 0.321-0.366, that correspond to the Class E (μ:0.25 to 0.35) and Class F (μ: 0.35 to 0.45). Friction materials have to be designed so that the coefficient of friction is maintained over a wide range of stressing condition.

Table 7: Experimental results and S/N ratio for wear and brake fade amount

Set	*W* (%)	S/N ratio (dB)	*f*	S/N ratio (dB)
1	2.36	-7.458	0.038	28.404
2	1.54	-3.750	0.050	26.021
3	2.50	-7.959	0.070	23.098
4	1.92	-5.666	0.075	22.499
5	3.05	-9.686	0.040	27.959
6	2.58	-8.232	0.075	22.499
7	2.69	-8.595	0.044	27.131
8	2.41	-7.640	0.051	25.849

W: Wear; *f*: Fade

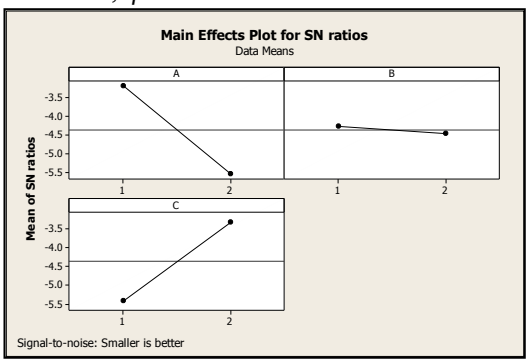

Figure 2 Main effect plots for S/N ratio for wear (*W*) and brake fade amount (*f*)

Table 7 shows experimental results of wear, fade amount and corresponding S/N ratio. In this experiment, smaller value of wear and brake fade amount are desirable. The smaller-the-better characteristics should be taken for obtaining optimal tribological behavior. Wear of friction materials should be minimized as much as possible. Higher wear rate means shorter friction material life and thus, incurred more material and maintenance cost. Lower wear rate would increase the life of the brake pad and higher friction coefficient would offer a better performance. Brake fade was related to thermal stability and thermal diffusivity of ingredients. Large amount of brake fade that organic ingredients decomposed at elevated temperature above 340^{o}C.

The category the-lower-the-better was used to calculate the S/N ratio for both quality characteristics wear (*W*) and fade performance (*f*), according to the equation:

$$S/N = -10\log\frac{1}{n}\left(\sum_{i=1}^{n} y_i^2\right) \qquad (2)$$

Based on the results in Table 7, analysis of the results leads to the graph in Figure 2 used to determine the optimal set of parameters from this experimental design. The control factor of molding pressure (A) at level 1 (50 tonnes) provided the best result. Molding pressure of 50 tonnes provide adequate bonding forces as an increase in pressure will cause an increase in energy waste. Similarly, the control factor of molding temperature (B) at level 1 (150^{o}C) provided the best result. This suggest that the wear and fade of friction material increases at high molding temperature was caused by resin decomposition (Lin and Ma, 2000). However, Kim et al., 2003 reported higher molding temperature in their study. Molding time (C) at level 2 (600 second) provided higher S/N ratio than at level 1 (300 second). Molding time of

300 second (C1) explained the insufficient time for the binding process and the weak binding of the phenolic resin between powders even though Ertan and Yavuz, 2010 claimed lower molding time. Figure 2 also shows that the molding pressure (A) has a greatest impact on tribological behavior followed by molding time (C) and finally, molding temperature (B).

Table 8 shows the results of ANOVA for wear, *W* and brake fade amount, *f*. It can be found that molding pressure (A) and molding time (C) are the significant manufacturing parameters for affecting wear and brake fade amount. Molding temperature (C) has an insignificant effect (p = 0.814). Therefore, the optimized combination of levels for the three control factors from the analysis was A1 (50 tonnes), B1 (150^{o}C) and C2 (600 second).

After identifying the optimal levels of all the control factors, the final stage is to verity the tribological properties by conducting the confirmation experiments. The condition A1B1C2 of the optimal parameters combination of the molding process was treated as confirmation run. Three specimens of friction materials were prepared under the optimal parameter set up in the study for the purpose of confirmation run. Table 9 indicates the results of the confirmation run. The mean wear of the confirmation specimens was 1.52% compared with the lowest measurements value in Table 7 was 1.54%. This result indicates that the selected control factor level produced the best wear characteristics.

Figure 3 exhibits the correlation among surface hardness, specific gravity and wear of the friction materials studied in this work. The figure clearly indicates that no apparent relationship between hardness and specific gravity or wear. This result point out that friction performance cannot be fully determined by only comparing the physical properties of friction materials. Tribological characteristics are the major determinant to best formulation that could be used as prototype while physical properties act as quality control for consistent composition in actual production process.

Table 8: Results of the ANOVA for wear (*W*) and brake fade amount (*f*)

Factor	Sum of squares	*F*-value	*p*-value
A	10.8394	10.13	0.033
B	0.0677	0.06	0.814
C	8.8169	8.24	0.045

Table 9: Results of the confirmation run

Specimen	*W* (%)
1	1.30
2	1.62
3	1.64
Mean	1.52

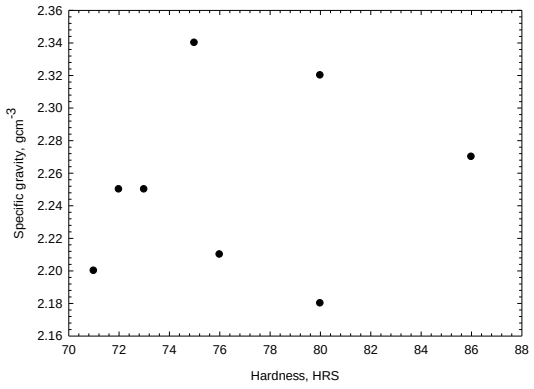

(a)

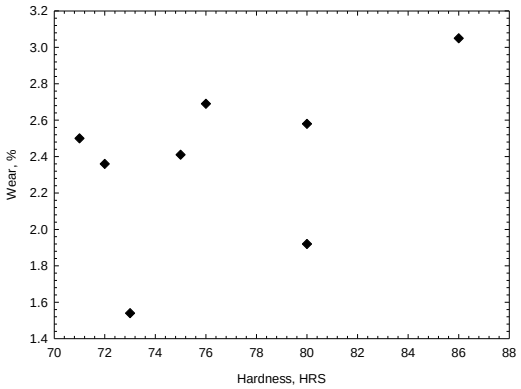

(b)

Figure 3 The relationship between physical properties: (a) hardness and specific gravity and (b) hardness and wear

4. CONCLUSION

This study presented an efficient method to determining the optimal manufacturing parameters for improved tribological behavior of friction materials through the use of Taguchi parameter design process. The analytical results are summarized as follows:

1. The molding pressure had the strongest influence on tribological characteristics. From the results evaluated, it was determined that the molding pressure should be held within the optimal limits.

2. The results summarised above suggest optimum manufacturing parameters for which the friction materials composition used in our experiments exhibited the best tribological properties with minimum energy waste. These optimal parameters are 50 tonnes molding pressure (A), 150^{o}C molding temperature (B), and 600 seconds molding time (C).
3. Tribological characteristics are the major determinant to best formulation that could be used as prototype while physical properties act as quality control for consistent composition in actual production process.

ACKNOWLEDGEMENT

The authors would to thank Advanced Materials Research Center, SIRIM Berhad, Malaysia for their technical assistance. Support from the Excellent Fund Universiti Teknologi MARA with the grant no: ST/DANA(39/09) is gratefully acknowledged.

REFERENCES

Al-Qureshi, H. A., Soares, M. R. F., Hotza, D., Alves, M. C., and Klein, A. N. 2008. Analyses of the fundamental parameters of cold die compaction of powder metallurgy. Journal of Materials Processing Technology, 199(1-3): 417-424.

Bijwe, J., Nidhi, Majumdar, N., and Satapathy, B. K. 2005. Influence of modified phenolic resins on the fade and recovery behaviour of friction materials. Wear 259: 1068-1078.

Cho, M. H., Kim, S. J., Kim, D., and Jang, H. 2005. Effects of ingredients on tribological characteristics of a brake lining: An experimental case study. Wear, 258(11-12): 1682-1687.

Ertan, R., and Yavuz, N. 2010. An experimental study on the effects of manufacturing parameters on the tribological properties of brake lining materials. Wear, 268(11-12): 1524-1532.

Esswein Junior, J. A. L., Arrieche, F. E., and Schaeffer, L. 2008. Analysis of wear in organic and sintered friction materials used in small wind energy converters. Materials Research, 11: 269-273.

Ibhadode, A. O. A., and Dagwa, I. M. 2008. Development of asbestos-free friction lining material from palm kernel shell. Journal of the Brazilian Society of Mechanical Sciences and Engineering, 30(2): 166-173.

Jang, H., Lee, J. S., and Fash, J. W. 2001. Compositional effects of the brake friction material on creep groan phenomena. Wear, 251(1-12): 1477-1483.

Kim, S. J., Kim, K. S., and Jang, H. 2003. Optimization of manufacturing parameters for a brake lining using Taguchi method. Journal of Materials Processing Technology, 136(1-3): 202-208.

Kim, Y. C., Cho, M. H., Kim, S. J., and Jang, H. 2008. The effect of phenolic resin, potassium titanate, and CNSL on the tribological properties of brake friction materials. Wear, 264(3-4): 204-210.

Kurt, A., and Boz, M. 2005. Wear behaviour of organic asbestos based and bronze based powder metal brake linings. Materials & Design, 26(8): 717-721.

Lin, J.-M., and Ma, C.-C. M. 2000. Thermal degradation of phenolic resin/silica hybrid ceramers. Polymer Degradation and Stability, 69(2): 229-235.

Tang, C. F., and Lu, Y. 2003. Optimization of an Industrial Friction Material Formulation. Tribology Transaction 46(1): 19-23.